

CHAPITRE 1: GLOBAL TRANSFORMS

IMAGE PROCESSING

GENERAL MODEL

The basic concept of any transform is to represent an image s (with pixel values $s(i,j)$) as weighted sum of basis images b_k (with pixel values $b_k(i,j)$).

$$s(i,j) = b_1(i,j) \text{coeff}(1,1) + b_2(i,j) \text{coeff}(1,2) + \dots + b_{NM}(i,j) \text{coeff}(N,N)$$

The matrix equation is: $s(i,j) = \sum_{k=1}^L \text{coeff}_k b_k(i,j)$ or $s(i,j) = \sum_{k=1}^L \sum_{l=1}^M \text{coeff}(k,l) b_{kl}(i,j)$

where: L is the number of basis images to represent the full image s
 $N \times N$ is the size of the original image and thus the number of basis vectors needs to perfectly represent it ($\mathbb{R}^{N \times N} = \text{span}\{v_i, i=1, \dots, N \times N \mid v = \sum \alpha_i v_i\}$)

forward transform $\rightarrow s$ corresponds to the spatial domain
 coeff: corresponds to the transformed domain \rightarrow inverse transform

The recipe for matrix to vector conversion is:

$$\begin{aligned} 2D \rightarrow 1D &: \begin{cases} s(m,n) \Rightarrow s(k) \\ k = m + (n-1)M \end{cases} \\ \text{vector to matrix conversion is: } 1D \rightarrow 2D &: \begin{cases} m = \text{mod}_M(k) \\ n = 1 + \lfloor \frac{k}{M} \rfloor \end{cases} \end{aligned}$$

The physical meaning of the expression into basis is the projection of s on a plane defined by b_i ($i=1, \dots, L$) linearly independent vectors to form $s' = \sum b_i \text{coeff}_i$.
 If b_i are orthogonal: $\text{coeff}_i = b_i^T \cdot s'$. To recover s from its projections on b_i , we need a number of linear independent vector b_i equal to the number of components of the vector s . Given: $s' = \underline{b} \text{coeff}$ and $s = \underline{b} \cdot \text{coeff}$ (from here derive k)

with $s': [P, 1]$; $b_k: [K, 1], k=1, \dots, L$; $\underline{b}: [P, L]$; $\text{coeff} [L, 1]$, if
 • $L = P$ ($L = N \times N$), it is always possible to define a set of linearly independent basis images so that no signal information is lost ($s = s'$)
 • $L < P$ ($L < N \times N$), signal information is lost ($s \neq s'$)

The goal of every transform is to minimize this error, generally through the minimization of the least square error: $LSE = \|s - s'\|^2 = (s - s')^T (s - s')$ and $\frac{\partial (LSE)}{\partial \text{coeff}} = 0$ for minimization, where LSE and coeff are vector following the

properties: $\frac{\partial (\underline{A} \cdot \text{coeff})}{\partial \text{coeff}} = \underline{A}^T$ and $\frac{\partial (\text{coeff}^T \cdot \underline{A})}{\partial \text{coeff}} = \underline{A}$

Demo:

$$\begin{aligned} LSE &= (s - s')^T (s - s') = s^T s - s^T \underline{b} \text{coeff} - \text{coeff}^T \underline{b}^T s + \text{coeff}^T \underline{b}^T \underline{b} \text{coeff} \\ \frac{\partial (LSE)}{\partial \text{coeff}} &= \begin{bmatrix} \frac{\partial (LSE)}{\partial \text{coeff}_1} \\ \vdots \\ \frac{\partial (LSE)}{\partial \text{coeff}_L} \end{bmatrix} = 0 - (s^T \underline{b})^T - (\underline{b}^T s) + (\underline{b}^T \underline{b} \text{coeff}) \\ &= -\underline{b}^T s - \underline{b}^T s + \underline{b}^T \underline{b} \text{coeff} + \underline{b}^T \underline{b} \text{coeff} \\ \Rightarrow \underline{b}^T \underline{b} \text{coeff} &= \underline{b}^T s \Rightarrow \text{coeff} = (\underline{b}^T \underline{b})^{-1} \underline{b}^T s = \underline{b}^T \end{aligned}$$

\therefore pseudo inverse of

Proof:

$A \in \mathbb{R}^{m \times n}, x \in \mathbb{R}^n$
 \rightarrow coeff is a vector in this case
 $A \cdot x \rightarrow$ product by rows of $A: \tilde{\alpha}_i$ (convention)
 column vector x
 if convention change result will be the transpose of the result found here.

Derive:

$$\frac{\partial A x}{\partial x} = \begin{bmatrix} \frac{\partial \tilde{\alpha}_1 x}{\partial x} \\ \vdots \\ \frac{\partial \tilde{\alpha}_m x}{\partial x} \end{bmatrix} = [\tilde{\alpha}_1 \tilde{\alpha}_2 \dots \tilde{\alpha}_m] = A^T$$

DISCRETE KARHUNEN LOEVE TRANSFORM

Let b_k be the eigenvectors and λ_k the corresponding eigenvalues of \underline{C}_s the covariance matrix $\left(= \frac{1}{K-1} \sum_{k=1}^K (s_k - m_s)(s_k - m_s)^T \right)$ where $m_s = \frac{1}{K} \sum_{k=1}^K s_k$ is the mean, and assume that the eigenvalues have been ordered in descending order: $\lambda_1 \geq \lambda_2 \geq \dots \geq \lambda_p$.

The Karhunen Loève transformation matrix is given by $\underline{b} = (b_1, b_2, \dots, b_p)$

The Discrete Karhunen Loève Transform is defined as: $\text{coeff} = \underline{b}^T (s - m_s)$

and calculate the L basis changes so that for each $L \leq p$, the $\text{MSE} := E(\|s - s'\|^2)$ between s and s' is minimal (where E is the expected value operator)

The properties of the DKLT are:

1) $m_{\text{coeff}} = 0$

2) $\underline{C}_{\text{coeff}} = \text{diag}(\lambda_1, \lambda_2, \dots, \lambda_p)$

3) the elements of coeff are uncorrelated

4) λ_i is equal to the variance of coeff_i along vector b_i

5) since \underline{C}_s is a real symmetric matrix, it is always possible to find a set of orthonormal eigenvectors. It therefore follows that s can be reconstructed as follows: $s = \underline{b} \text{coeff} + m_s$ (inverse KLT)

6) if $L < p$, $s \approx \underline{b}_L \text{coeff} + m_s$ ($\underline{b}_L = (b_1, \dots, b_L, 0, \dots, 0)$), the MSE is given by

$$\text{MSE} = \sum_{j=L+1}^p \lambda_j = \sum_{j=L+1}^p \lambda_j$$

→ or $\text{coeff} = (\text{coeff}_1, \text{coeff}_2, \dots, 0, \dots, 0)$
thus we either zero out the basis or the coefficients.

Proofs of properties

Assumptions:

- Let s be a square image: $[N^2, 1]$ and s' be: $[L, 1]$ with $\begin{cases} L \leq N^2 \\ E(s) = 0 \\ E(s') = 0 \end{cases}$
- We impose that $E(\|s - s'\|^2)$ is minimal $\forall L$
- The basis \underline{b} is orthonormal: $\underline{b}^T \underline{b} = \underline{I}$

1) $m_{\text{coeff}} = E(\text{coeff}) = E(\underbrace{\underline{b}^T}_{\substack{\text{deterministic,} \\ \text{not of expectation} \\ \text{operator}}} (s - m_s)) = \underbrace{\underline{b}^T}_{=: m_s} (E(s) - m_s) = 0$

3) As \underline{C}_s is diagonal, the diagonal terms are zero thus the non-correlation is zero, hence they are uncorrelated.

6) In the case where $L = N^2$,
 $\underline{C}_s = E(ss^T) = \begin{bmatrix} \sigma_s^2(1) & \dots & \text{other terms} \\ \vdots & & \sigma_s^2(N^2) \end{bmatrix}$
 $\underline{C}_{\text{coeff}} = E(\text{coeff} \text{coeff}^T) = \begin{pmatrix} \sigma_{\text{coeff}}^2(1) & \dots & \text{other terms} \\ \vdots & & \sigma_{\text{coeff}}^2(N^2) \end{pmatrix}$
 $= E(\underline{b}^T s s^T \underline{b}) = \underline{b}^T E(ss^T) \underline{b} = \underline{b}^T \underline{C}_s \underline{b}$

thus $\text{tr}(\underline{C}_s) = \text{tr}(\underline{C}_{\text{coeff}}) = \sum_{i=1}^{N^2} \sigma_{\text{coeff}}^2(i)$ is basis invariant

In the case where $L \leq N^2$ and in the case we zero out some coefficients.

$\underline{C}_{\text{coeff}}' = \begin{bmatrix} \sigma_{\text{coeff}}^2(1) & \dots & \text{other terms or 0} & 0 \\ \vdots & & \sigma_{\text{coeff}}^2(L) & 0 \\ 0 & & 0 & 0 \end{bmatrix}$ then $\text{tr}(\underline{C}_{\text{coeff}}') = \text{tr}(\underline{C}_s) - (\sigma_{\text{coeff}}^2(L+1) + \dots + \sigma_{\text{coeff}}^2(N^2))$

we have as:

$$E(\|s - s'\|^2) = E((s - s')^T (s - s')) = \underbrace{E(s^T s)}_1 + \underbrace{E(s'^T s')}_2 - \underbrace{E(s^T s')}_3 - \underbrace{E(s'^T s)}_4$$

1. $E(s^T s) = E(s^2/1 + \dots + s^2/N^2) = \sigma_s^2/1 + \dots + \sigma_s^2/N^2 = \text{tr}(C_s)$ represents the energy of s

$E(s^T s) = E((b \cdot \text{coeff})^T (b \cdot \text{coeff})) = E(\text{coeff}^T \underbrace{b^T b}_{I} \text{coeff}) = E(\text{coeff}^T \text{coeff}) = \text{tr}(C_{\text{coeff}})$

2. $E(s'^T s') = E((b \cdot \text{coeff}')^T (b \cdot \text{coeff}')) = \text{tr}(C_{\text{coeff}'})$ only valid for orthonormal b because $b^T b = I$

3. $E(s^T s') = E((b \cdot \text{coeff})^T (b \cdot \text{coeff}')) = E(\text{coeff}^T b^T b \text{coeff}') = E(\text{coeff}^T \text{coeff}')$
 $= E(\text{coeff}^2/1 + \dots + \text{coeff}^2/L) = \sigma_{\text{coeff}}^2/1 + \dots + \sigma_{\text{coeff}}^2/L = \text{tr}(C_{\text{coeff}'})$

4. $E(s'^T s) = E((b \cdot \text{coeff}')^T (b \cdot \text{coeff})) = \text{tr}(C_{\text{coeff}'})$

* the results $\text{tr}(C_s) = \text{tr}(C_{\text{coeff}})$ means that the energy in time domain is conserved in the transform domain C_{coeff} . This follows the Parseval theorem.

$$= \text{tr}(C_{\text{coeff}}) + \text{tr}'(C_{\text{coeff}'} - \text{tr}(C_{\text{coeff}'} - \text{tr}(C_{\text{coeff}'}))$$

$$= \text{tr}(C_{\text{coeff}}) - \text{tr}(C_{\text{coeff}'})$$

by using of property 3) $\rightarrow \sigma_{\text{coeff}}^2(L+1) + \dots + \sigma_{\text{coeff}}^2(N^2)$ and this should be minimum

Because the energy is fixed, it means that $\sigma^2/1 + \dots + \sigma^2/L$ should have a maximum energy. The minimization of the NSE also impose that the variance of the projection of s on \underline{b} should be maximum. As an example, if $L = 1$:

$\sigma^2 \text{coeff}(1) = C_{\text{coeff}}(1,1) = b_1^T C_s b_1$ to be max $\xrightarrow{\text{derivative}} \frac{d}{db_1} (b_1^T C_s b_1 - \lambda(b_1^T b_1 - 1)) = 0$
 $b_1^T b_1 = 1$ by constraint of orthonormal basis

By $\frac{\partial(Ax)}{\partial x} = A^T$: $\frac{d}{db_1} (b_1^T (C_s - \lambda I) b_1) = (b_1^T (C_s - \lambda I))^T$

By $\frac{\partial(x^T A)}{\partial x} = A$: $\frac{d}{db_1} (b_1^T (C_s - \lambda I) b_1) = (C_s - \lambda I) b_1$

$(b_1^T (C_s - \lambda I))^T + (C_s - \lambda I) b_1 = (C_s - \lambda I)^T b_1 + (C_s - \lambda I) b_1$

$= 2(C_s b_1 - \lambda b_1) = 0$ as $C_s = C_s^T$ because C_s is symmetric.

$\Rightarrow C_s b_1 = \lambda b_1 \rightarrow b_1$ is an eigenvector of C_s and as $b_1^T C_s b_1$ must be max, b_1 must be the eigenvector with the largest possible eigenvalue λ_1 . By generalizing, λ_2 and the following should be the next -- highest eigenvalues such that $C_s b = \underline{b} \Lambda$ where $\Lambda = \begin{bmatrix} \lambda_1 & & \\ & \ddots & \\ & & \lambda_L \end{bmatrix}$ with $\lambda_1 \geq \lambda_2 \geq \dots \geq \lambda_L$.

The DKLT is constructed iteratively by finding these largest eigenvalues to minimize the NSE. Indeed, because the eigenvector dropped corresponds to the last eigenvalues and as these last eigenvalues are always the smallest, the DKLT is a way to get the smallest possible. As a conclusion, the DKLT is a way to find the b_i orthonormal (\underline{b} is unitary, $\underline{b}^T \underline{b} = I$, $b_i b_j^T = \delta_{ij}$) as eigenvectors of a real symmetric matrix C_s . The coefficients are computed as $C_{\text{coeff}} = b^T C_s b = b^{-1} b \Lambda = I \Lambda = \Lambda$ is a diagonal matrix. The coefficients are ordered by decreasing variance and the reconstruction error is exactly a minimum NSE $\forall L$.

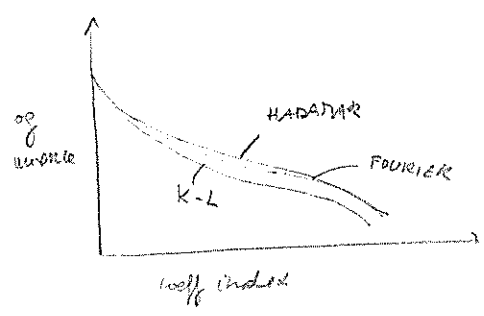
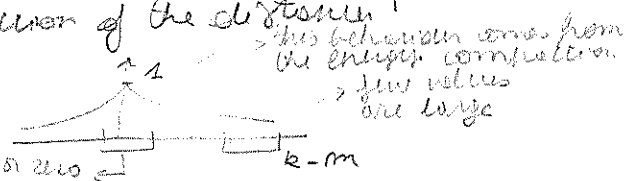
to solve the problem of compression of big data or images, we partition them into smaller partitions with the assumption that if the pixels are far or if they are neighbours but belonging to different partition, they are not correlated. The variance is an exponential function of the distance:

$$C(k, l)(m, n) = e^{-0,125 |k-m| - 0,243 |l-n|}$$

// $F_X(x) = \frac{1}{2} e^{-\lambda |x|}$ Laplace distribution many values are lower zero $e^{-\lambda |x|}$

the transformation is done independently for every partition and every partition has the same KLT images and eigenvalues

The DKLT gives the best efficiency curve for ensemble of images but the problem is that it is complex to implement as well as hard to be put while for other transforms, only the coeffs are sent. Moreover, the Fourier/DCT transform achieve almost same results with simpler implementation. Thus the KLT is a theoretical maximum.



Definitions

1-D IDFT $s(i) = \sum_{k=0}^{N-1} \text{coeff}_s(k) b_k(i)$ with $b_k(i) = \frac{1}{\sqrt{N}} e^{j2\pi i k / N}$

1-D DFT $\text{coeff}_s(k) = \sum_{i=0}^{N-1} s(i) b_k^*(i)$ with $b_k^*(i) = \frac{1}{\sqrt{N}} e^{-j2\pi i k / N}$

2-D IDFT $s(i, j) = \sum_{k=0}^{N-1} \sum_{l=0}^{N-1} \text{coeff}_s(k, l) b_k(i) b_l(j)$ with $b_{kl}(i, j) = b_k(i) b_l(j) = \frac{1}{N} e^{j2\pi(i k + j l) / N}$

2-D DFT $\text{coeff}_s(k, l) = \sum_{i=0}^{N-1} \sum_{j=0}^{N-1} s(i, j) b_k^*(i) b_l^*(j)$ with $b_{kl}^*(i, j) = b_k^*(i) b_l^*(j) = \frac{1}{N} e^{-j2\pi(i k + j l) / N}$

Starting from $s(i, j)$, if N is finite, $\text{coeff}_s(k, l)$ always exists. This can be verified by replacing 1-D DFT into 2-D IDFT and making use of the orthogonality property of the basis functions. A similar property exists for the continuous Fourier transform ($X(\omega) = \int x(t) e^{j\omega t} dt$) where the existence is guaranteed if the spectral image function is square integrable, i.e. the signal must be of finite energy.

$\text{coeff}_s(k, l) = \text{coeff}_{RE}(k, l) + j \text{coeff}_{IM}(k, l)$ or/ET $\text{coeff}_s(k, l) = |\text{coeff}_s(k, l)| \exp(j\phi(k, l))$ where

$|\text{coeff}_s(k, l)| = \sqrt{(\text{coeff}_{RE}(k, l))^2 + (\text{coeff}_{IM}(k, l))^2}$ and $\phi(k, l) = \tan^{-1} \left(\frac{\text{coeff}_{IM}(k, l)}{\text{coeff}_{RE}(k, l)} \right)$

↳ source amplitude spectrum

↳ phase spectrum

the power spectral density is $\Psi(k, l) = |\text{coeff}_s(k, l)|^2$

Properties

① Symmetric separability

② Linearity: $s_1(i, j) + s_2(i, j) \Leftrightarrow \text{coeff}_{s_1}(k, l) + \text{coeff}_{s_2}(k, l)$
 $a \cdot s(i, j) \Leftrightarrow a \cdot \text{coeff}_s(k, l)$

③ Scaling: $s(ai, bj) \Leftrightarrow \frac{1}{ab} \text{coeff}_s\left(\frac{k}{a}, \frac{l}{b}\right)$

④ Translation in spatial/frequency domain: $s(i-i_0, j-j_0) \Leftrightarrow \text{coeff}_s(k, l) \exp\left(\frac{j2\pi(k i_0 + l j_0)}{N}\right)$
 $s(i, j) \exp\left(\frac{j2\pi(i k_0 + j l_0)}{N}\right) \Leftrightarrow \text{coeff}_s(k-k_0, l-l_0)$

Demo:

① $\sum_{i=0}^{N-1} \sum_{j=0}^{N-1} (s_1(k, l) + s_2(k, l)) b_k^*(i) b_l^*(j) = \sum_{i=0}^{N-1} \sum_{j=0}^{N-1} (s_1(k, l) b_k^*(i) b_l^*(j) + s_2(k, l) b_k^*(i) b_l^*(j))$
 $= \sum_{i=0}^{N-1} \sum_{j=0}^{N-1} s_1(k, l) b_k^*(i) b_l^*(j) + \sum_{i=0}^{N-1} \sum_{j=0}^{N-1} s_2(k, l) b_k^*(i) b_l^*(j) = \text{coeff}_{s_1}(k, l) + \text{coeff}_{s_2}(k, l)$

② $\sum_{i=0}^{N-1} \sum_{j=0}^{N-1} s(ai, bj) \frac{1}{N} e^{-j2\pi(i k + j l) / N}$ let $i' = ai$ $j' = bj$
 $\sum_{i'=0}^{(N-1)a} \sum_{j'=0}^{(N-1)b} s(i', j') \frac{1}{N} e^{-j2\pi(i' k/a + j' l/b) / N} = \frac{1}{|ab|} \text{coeff}_s\left(\frac{k}{a}, \frac{l}{b}\right)$

$s(i-i_0, j-j_0) = \sum_{k=0}^{N-1} \sum_{l=0}^{N-1} \text{coeff}_s(k, l) b_k(i-i_0) b_l(j-j_0) = \sum_{k=0}^{N-1} \sum_{l=0}^{N-1} \text{coeff}_s(k, l) \frac{1}{N} e^{j2\pi((i-i_0)k + (j-j_0)l) / N}$
 $= \sum_{k=0}^{N-1} \sum_{l=0}^{N-1} \text{coeff}_s(k, l) \frac{1}{N} e^{j2\pi(i k + j l) / N} e^{-j2\pi(i_0 k + j_0 l) / N} = \sum_{k=0}^{N-1} \sum_{l=0}^{N-1} \text{coeff}_s(k, l) \frac{1}{N} e^{j2\pi(i k + j l) / N} e^{-j2\pi(i_0 k + j_0 l) / N}$

③ Periodicity: $\text{coeff}_s(k, l) = \text{coeff}_s(k+N, l) = \text{coeff}_s(k, l+N) = \text{coeff}_s(k+N, l+N)$

If we apply the inverse transform, we obtain a periodic function $s_p(i, j)$ from which one period is equal to $s(i, j)$.

1) Conjugate symmetry: if $s(i,j)$ is real $\Rightarrow \text{coeff}_s(k,l) = \text{coeff}_s^*(-k,-l)$ (conjugate symmetry)
 $|\text{coeff}_s(k,l)| = |\text{coeff}_s(-k,-l)| < \phi(k,l) = -\phi(-k,-l)$
 using properties 4 & 5 in normalization: $k_0 = l_0 = \frac{N}{2}$: $s(i,j) (-1)^{i+j} \Leftrightarrow \text{coeff}_s(k - \frac{N}{2}, l - \frac{N}{2})$

2) If $s(i,j)$ is rotated over an angle θ then $\text{coeff}_s(k,l)$ is rotated over the same angle θ
 for discrete images, this is only approximately true: a pixel is not mapped to a new pixel position after rotation. Rotation of a discrete image automatically involves interpolation as pixel at position $\text{pixel} + \theta$ might not exist.

3) Assume $sl(i,j)$ is the Laplacian ($s(i,j)$ in freq domain): $sl(i,j) \Rightarrow \left(\frac{2\pi}{N}\right)^2 (k^2 + l^2) \text{coeff}_s(k,l)$
 the Laplacian emphasizes high frequency components and hence it also enhances edges

Proof:

$$\Rightarrow s(i,j) \cdot e^{j\theta} \Rightarrow \sum_k \sum_l \text{coeff}_s(k,l) b_k(i) b_l(j) e^{j\theta} = \sum_k \sum_l \left[\text{coeff}_s(k,l) \cdot e^{j\theta} \right] b_k(i) b_l(j)$$

$$\textcircled{2} \Delta s(i,j) = \frac{\partial^2 s(i,j)}{\partial i^2} + \frac{\partial^2 s(i,j)}{\partial j^2} \text{ and } \frac{\partial^2 s(i,j)}{\partial i^2} = \sum_k \sum_l \text{coeff}_s(k,l) \frac{1}{N} \frac{\partial^2}{\partial i^2} \left(e^{\frac{j2\pi(i+k)}{N}} \right)$$

$$\text{and } \frac{\partial}{\partial i} \left(e^{\frac{j2\pi i k}{N}} \right) = e^{\frac{j2\pi i k}{N}} \frac{j2\pi k}{N} \Rightarrow \frac{\partial^2}{\partial i^2} \left(e^{\frac{j2\pi i k}{N}} \right) = e^{\frac{j2\pi i k}{N}} - \left(\frac{2\pi}{N} \right)^2 k^2 e^{\frac{j2\pi i k}{N}}$$

by doing same with $\frac{\partial^2}{\partial j^2}$ we obtain: $\Delta s(i,j) = \sum_k \sum_l \text{coeff}_s(k,l) \underbrace{\left(-\left(\frac{2\pi}{N} \right)^2 (k^2 + l^2) \right)}_{\text{COFD}} b_k(i) b_l(j)$

Display of Fourier Coefficient Images
 The $\text{coeff}_s(m,n)$ have a high dynamic range. The image spectrum usually differs very rapidly with increasing frequency but the high frequency components are important since they are mainly due to sharp transitions. To adapt the content in the displayed image to the dynamic range of the display and the eye, a logarithmic rule is applied on the coefficients:

$$\text{disp}(m,n) = \log(1 + |\text{coeff}_s(m,n)|) \geq 0 \quad (\text{disp}(m,n) = 0 \Rightarrow \text{coeff}_s(m,n) = 0)$$

$$\frac{F_{\max}}{F_{\min}} \rightarrow R = \frac{\log 1 + K F_{\max}}{\log 1 + K F_{\min}}$$

is it possible?

Definitions

1-D IDCT $s(i) = \sum_{k=0}^{N-1} \text{coeff}_k(k) \cos(ki)$ with $\cos(ki) = c(k) \cos \frac{(2i+1)k\pi}{2N}$, $c(k) = \begin{cases} \frac{1}{\sqrt{N}} & \text{for } k=0 \\ \frac{\sqrt{2}}{\sqrt{N}} & \text{for } k=1 \dots N \end{cases}$

1-D DCT $\text{coeff}_k(k) = \sum_{i=0}^{N-1} s(i) \cos(ki)$ with $\cos(ki) = c(k) \cos \frac{(2i+1)k\pi}{2N}$

2-D IDCT $s(i,j) = \sum_{k=0}^{N-1} \sum_{l=0}^{N-1} \text{coeff}_{kl}(k,l) \left(c(k) \cos \frac{(2i+1)k\pi}{2N} \right) \left(c(l) \cos \frac{(2j+1)l\pi}{2N} \right)$

2-D DCT $\text{coeff}_{kl}(i,j) = \sum_{k=0}^{N-1} \sum_{l=0}^{N-1} s(k,l) \left(c(k) \cos \frac{(2k+1)i\pi}{2N} \right) \left(c(l) \cos \frac{(2l+1)j\pi}{2N} \right)$

Some questions

slide 63 & 64 is incorrect !!!

- pg 64 note (d) should be zero

USE of DCT

The cosine transform is almost as good as the KCL without having to shift the loads and compute it, as it is already pre-shifted. Only the coefficients have to be sent.

improved resolution

Applications

Noise reduction

through the appropriate choice of a limited set of basis images and projection of the measured image on this subset of basis images, noise reduction may be obtained (if course within limits). Indeed, typical images show large spread energy contributions at low frequencies and decreasing towards high frequencies while noise has a broad spectrum. As a result of this, generally, the SNR at high frequencies is much lower than at low frequencies. The goal of the projection is then to retain the low frequency components of the measured image, i.e. the projection of the measured image on the basis of low basis images.

Transformation to a feature space

Sometimes the basis images and/or their associated coefficients carry a physical interpretation.

→ coefficients: in the case where the basis images have been fixed a priori and have not been derived from the data itself (KLT), only the coefficients are meaningful. Ex: in FT (Fourier), the frequency spectrum allows for analysis of the amplitude, the phase and the energy distribution.

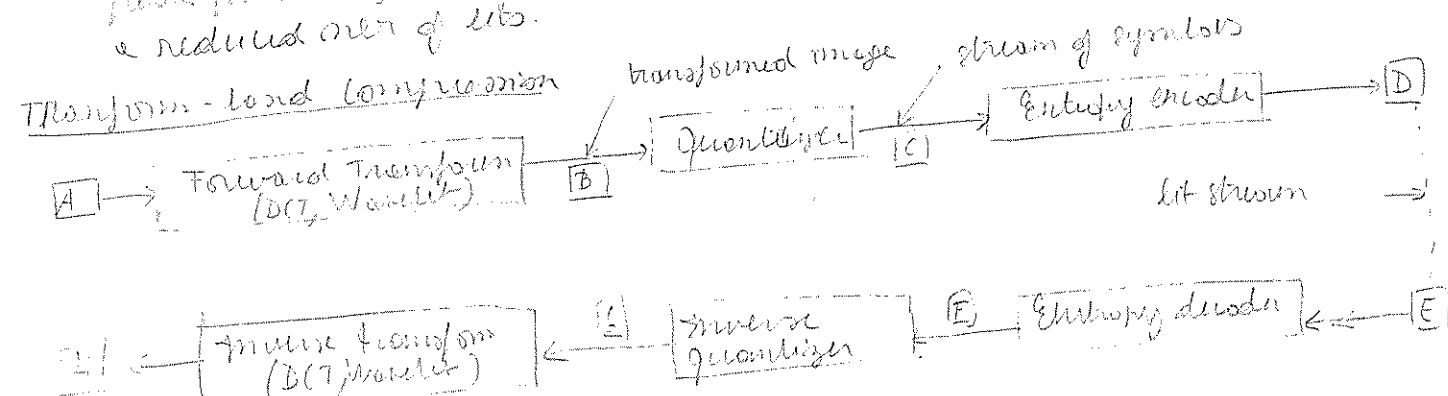
→ basis images: in the case where the basis images are derived from data, both coeff & basis images are meaningful. Ex: KLT.

Data compression

Since neighbouring grey values in an image with $N \times N$ pixels are usually highly correlated, data compression must be possible. In global transforms, the image is written as a weighted sum of L basis images. These basis images are considered as the atoms as they can either be calculated for a set of representative images (KLT) or precalculated a priori (DFT, DCT, WHT). Hence, each individual image is characterized by the set of L weighting coefficients which can be stored in a new image. The transformed image itself can be stored in a new image. The transformation occurs but there is no data compression.

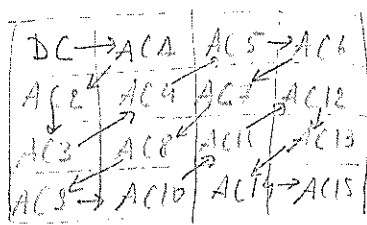
→ if $L = N^2$ no loss of information occurs but there is no data compression.

→ if $L < N^2$ there is loss of information and data compression which is most efficient for coefficients with low mutual correlation (i.e. if coeff are uncorrelated, the original number of coeff is reduced) and with low variance (i.e. a peak probability density function) with this low coding (quantization) with a reduced number of bits.



Ex: DCT based encoder

5



DC components <
AC components for the
DCT of the 4x4 blocks

- partition of the input image into blocks
- Apply the DCT transform on $N \times N$ blocks
- Apply scalar quantization of the DCT coefficients
- Scan and entropy encode the resulting quantization modules

→ scanning order to be defined (here by \rightarrow)

Resolution scalability:

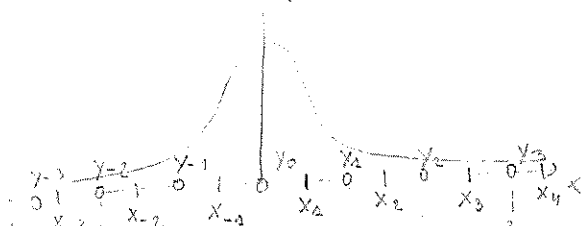
To obtain resolution scalability, multiresolution transforms such as wavelet transform can be used. Progressively sending the wavelets subbands from lowest to highest resolution level naturally provides resolution scalability. (cf. section 5.4 slide 86/124 in part 3 - notes):

- sending & decoding only the lowest resolution LL subband (corner top left) corresponds to the lowest resolution version of the original image
Ex: Lena is small in top-left subband: resolution is $1/16$ of the original both horizontally and vertically
- sending 3 high frequency subbands next to the LL subband (having each the same number of samples as the LL subband) and performing a one level inverse wavelet transform will enable reconstructing a higher resolution version of the image, which will have a resolution twice as large as the LL subband on both dimension ($1/8$ of the original resolution)

The DCT transform can also be used to provide resolution scalability. Say each DCT block has $N \times N$ samples, each DCT coefficient corresponds to a specific horizontal and vertical frequency. The top left corner corresponds to the DC component. If you send only $\frac{N}{2} \times \frac{N}{2}$ DCT coefficients in each block and perform an $\frac{N}{2} \times \frac{N}{2}$ inverse DCT transform, will give you an image which is half the size of the original image both horizontally and vertically.

SCALAR QUANTIZATION

$\wedge p_X(x)$



if $x_{i-1/2} \leq x < x_{i+1/2} : \hat{Q}(x) = y_i, i \geq 1$

if $x_{-1/2} \leq x < x_{1/2} : \hat{Q}(x) = 0$

x_i : decision points

$[x_i, x_{i+1})$: uncertainty interval

y_i : reconstruction points

$(x_{i-1/2}, x_{i+1/2})$: decision interval \rightarrow all points are mapped to y_i and seen the distribution, lots of chance to observe a given

$$p_Y(i) = P(Y=y_i) = \int_{x_{i-1/2}}^{x_{i+1/2}} p_X(x) dx$$

$$Q^{-1}(i) = y_i \Rightarrow Q^{-1}(Q(x)) = y_i$$

Based on a given distribution, the quantizer is chosen such that it minimizes the mean square distortion given by:

$$D_n = \sum_{i=1}^N \int_{x_{i-1/2}}^{x_{i+1/2}} (x - y_i)^2 p_X(x) dx$$

sum over all intervals \rightarrow min the distortion (error) \rightarrow choose of occurrence of the distribution

Such quantizers are called Lloyd-Max quantizers and satisfy:

$$\int_{x_{i-1/2}}^{x_{i+1/2}} (x - y_i)^{m-1} p_X(x) dx = \int_{y_i}^{x_{i+1/2}} (x - y_i)^{m-1} p_X(x) dx$$

$$\text{for } m=1 : \int_{x_{i-1/2}}^{x_{i+1/2}} p_X(x) dx = \int_{y_i}^{x_{i+1/2}} p_X(x) dx = \frac{1}{2} \int_{x_{i-1/2}}^{x_{i+1/2}} p_X(x) dx$$

$$m=2 : x_{i-1/2} = y_{i-1} + y_i, \quad k=1, 2, \dots, N-1 \quad (x_k \text{ are decision points})$$

$$y_k = \frac{\int_{x_{k-1/2}}^{x_{k+1/2}} x p_X(x) dx}{\int_{x_{k-1/2}}^{x_{k+1/2}} p_X(x) dx} \quad k=0, 1, \dots, N-1 \quad (y_k \text{ are centroids}) \quad (**)$$

However, Lloyd-Max quantizers are not optimal in the entropy coded case. Because the distortion rate, after coding the quantized values, is $R = H(Y) = -\sum_{i=1}^N p_Y(i) \log_2 p_Y(i)$. So instead, in this case, the optimal quantizer should minimize the MSE, subject to a constraint on the entropy:

$$J(\lambda) = \left(\sum_{i=1}^{N-1} \int_{x_{i-1/2}}^{x_{i+1/2}} (x - y_i)^2 p_X(x) dx - \lambda \sum_{i=1}^{N-1} \int_{x_{i-1/2}}^{x_{i+1/2}} p_X(x) dx \left(\log_2 \int_{x_{i-1/2}}^{x_{i+1/2}} p_X(x) dx \right) \right)$$

$D_2 \rightarrow \text{MSE}$

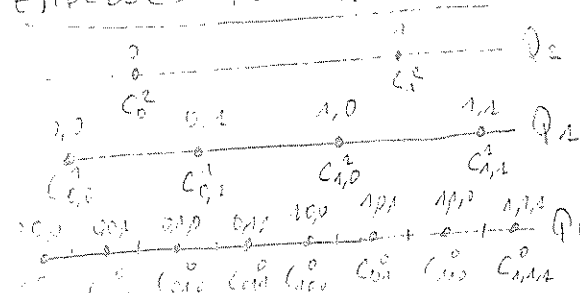
constraint on entropy

$$\frac{\partial J}{\partial y_k} = 0 \Rightarrow y_k = \text{result} \quad (**) \quad \text{and} \quad \frac{\partial J}{\partial \lambda} = 0 \Rightarrow (x_k - y_{k-1})^2 - (x_k - y_k)^2 - \lambda (\log_2 p_Y(i-1) - \log_2 p_Y(i)) = 0$$

\rightarrow iterative algorithm for solution

At high rates (large N) and for smooth pdf, the simplest quantizer which is optimal or close to the optimum in MSE sense is the uniform quantizer, as at high rates, the intervals $x_i - x_{i+1}$ are small and the pdf can be seen as uniform. In this case: $D_2 = \frac{\Delta^2}{12}$ ($\Delta = x_{N+1/2} - x_{-1/2}$) (can be found by replacing p_X of uniform dist. in formula of D_n with $m=2$) (embedded among each two contours gives one)

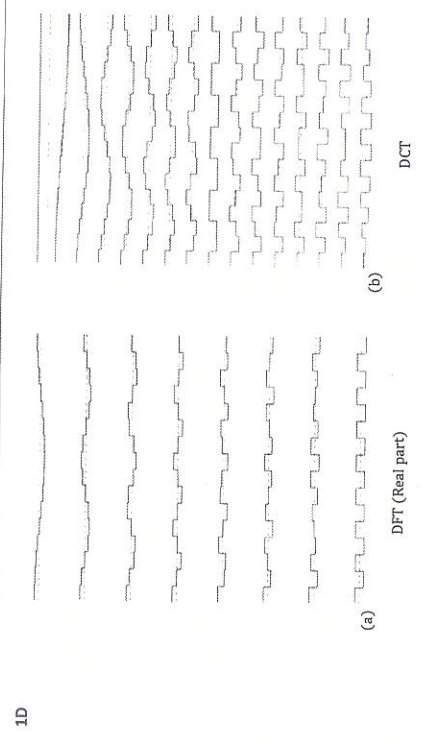
EMBEDDED QUANTIZATION



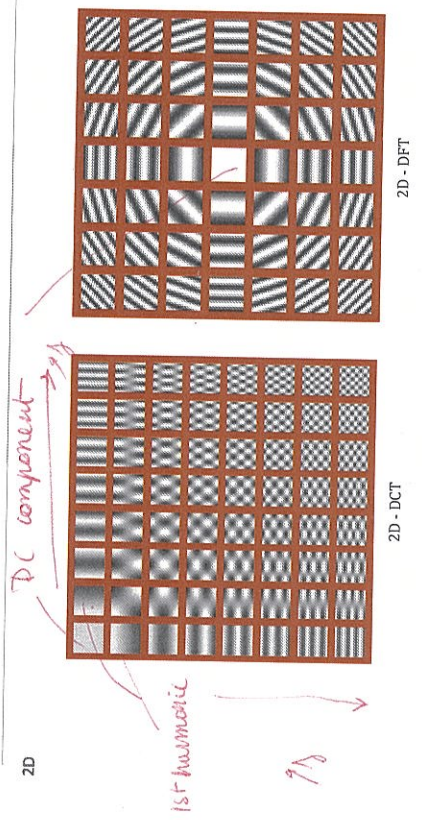
At various rates of quantizers $\hat{Q} = \{\hat{Q}_N, \hat{Q}_{N-1}, \dots, \hat{Q}_0\}$ with $\hat{Q}_N(x) = k_N, \hat{Q}_{N-1}(x) = k_N, k_{N-2}, \dots, \hat{Q}_0(x) = k_N, k_{N-1}, \dots, k_0$

At every step, the previous code k_N is refined to k_N, k_{N-1} until the previous level is added is needed. Such quantizers allow adaptation of the scheme to the available rate.

Basis functions for DFT and DCT

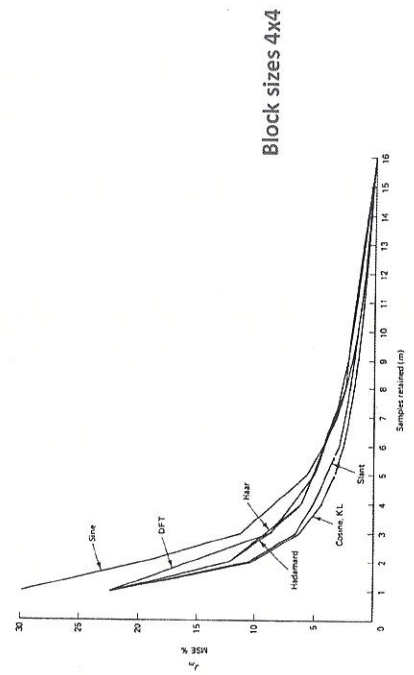


Basis functions for DFT and DCT

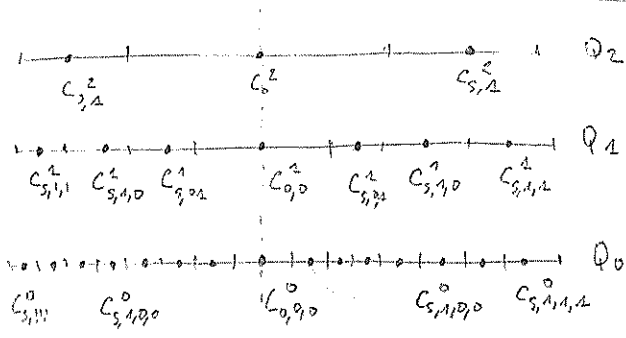


DCT = real part of DFT, it is a 2D separable transform but not symmetric. It compacts energy in a few components

Mean Square Error of truncation compression



1) BE BDE D DE AND ONE SCALAR IDENTIFICATION \rightarrow cf. exercise 11.10.10 p. 33.



$$Q_2(n) = 2, 1 / Q_1(n) = 5, 1, 0 / Q_j(n) = 2, 1, 0, 0$$

Approved use of such prioritizers:

quantization: $q_p = Q_p(x) = \begin{cases} \text{sign}(x) \left\lfloor \frac{|x|}{2^p \Delta} + \frac{\xi}{2^p} \right\rfloor & \text{if } |x| \geq \frac{\xi}{2^p} \\ 0 & \text{else} \end{cases}$

Matrix priorization: $y_i^P = \begin{cases} 0 & \text{if } i \neq p \\ \text{sign}(i-p) \left(|i-p| - \frac{\epsilon}{2P} + \delta \right) 2^P \Delta y_i^P & \text{if } i = p \end{cases}$

where, $\xi < 1$ controls the size of deadzone
 $0 \leq \delta < 1$ controls the placement of the reconstruction points in their respective cells.

$$i_0 = \varphi_0(x) \text{ and } i_0 = \operatorname{sign}(i_0) \sum_{j=0}^{N-1} 2^j k_j$$

$$1, k_{N-1}, k_{N-2}, \dots, k_{p-2}, \dots, k_1, k_0$$

it can be obtained by dropping the p least significant exponents from i_0 .

proof: writing ϵ from definition: $\left| \frac{1}{n} \right| = \left| \frac{1}{n} \right| + \left| \frac{\epsilon}{n} \right|$ and choosing p least square error

$$i_j^p = \text{sign}(i_0) \left\lfloor \frac{|i_0|}{2^p} \right\rfloor = \text{sign}(i_0) \left\lfloor \frac{|x|}{\Delta} + \frac{\xi}{2^p} \right\rfloor \text{ and by lemma } \left\lfloor \frac{|x|}{\Delta} + \frac{\xi}{2^p} \right\rfloor = 2^p m + n, m \in \mathbb{Z}, 0 \leq n < 2^p$$

~~$\text{sign}(io) = \text{sign}(io)$ and by using $\frac{|x|}{\Delta} + \frac{\epsilon}{\delta} = \left\lfloor \frac{|x|}{\Delta} + \frac{\epsilon}{\delta} \right\rfloor + \epsilon$, $0 \leq \epsilon < 1$

$= \text{sign}(X) \left\lfloor \frac{2^p m + n + \epsilon}{2^p} \right\rfloor = \text{sign}(X) \cdot m$

... the least non-negative~~

Here the quantization level p (p) is obtained by dropping the least \log_2 significant bits from the binary representation of x .

SUCCESSIVE APPROXIMATION QUANTIZATION

SUCCESSIVE APPROXIMATION (SQA) [11]
 Some schemes or undirected disjunctive scales priorization and some formulas tell
 with $\xi = 0$ and $\delta = \frac{1}{2}$ in the definitions. SQA can be simply implemented via
 thresholding, by applying a monotonically decreasing set of thresholds of the
 form: $t_{p-1} = \frac{I_p}{2}$

$$\text{form: } T_{p-2} = \frac{Tr}{2}$$

SCALABLE CODING \rightarrow this Analogous to P18.

quality stable - report on production

↳ apply same steps on pg 5 auto

to improve quality by taking more
quantization steps (augmented precision)
w/ a fixed nbr of DCT coefficients

A high conversion rate induces "belonging effect"

Resolution available \rightarrow 1 bit/pixel

→ apply same steps as pg 5 with

→ improve resolution by taking more DCT coefficients: ... for a fixed number of quantisation steps.

Los gr pg 5

CHAPTER 2: HOUGH TRANSFORM

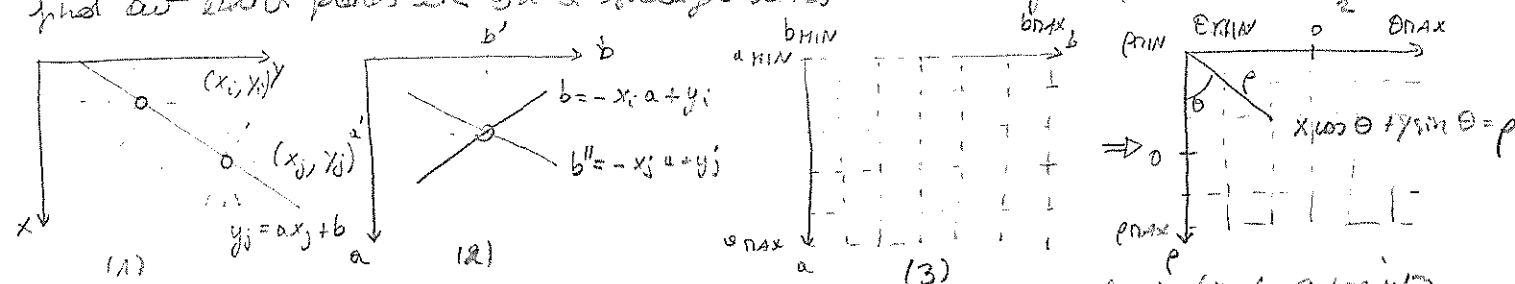
INTRODUCTION

The Hough Transform is a curve detection technique that can replace edge linking techniques by defining an algorithm that discovers the line between aligned points defining an edge. The algorithm works on a thresholded (i.e. binary) edge image. The advantage is that results are almost unaffected by gaps and by noise on the centers.

CASE: STRAIGHT LINES

To define a straight line, 2 approaches exist:

- find all lines determined by sets of 2 points number of lines: $\frac{n(n-1)}{2} \sim n^2$
- find out which points lie on a straight line number of comparisons: $\frac{n^2(n-2)}{2} \sim n^3$



The basic principle of the Hough Transform comes from the fact that 2 points (x_i, y_i) and (x_j, y_j) in aligned of (a, b) the line parameters method for both of them. This corresponds to an intersection in the (a, b) space. Indeed:

- The point (x_i, y_i) : $y_i = ax_i + b$ equation in (x, y) space
 $b = -x_i a + y_i$ equation in (a, b) space
- The point (x_j, y_j) : $y_j = ax_j + b$ equation in (x, y) space
 $b'' = -x_j a + y_j$ equation in (a, b) space

In the (a, b) space distinctified of the Hough Transform (3), the unit of the values of x_i, y_i showing the same (a, b) give the number of points showing the same (a, b) i.e. lying on the same line in the (x, y) space. However, which value to take to $a_{min}, b_{min}, a_{max}$ and b_{max} is not clear as they might go from $-\infty$ to $+\infty$. The polar representation of a line solves this problem: $0 \leq \theta < \pi$, $-\infty < \rho \leq +\infty$.

- The algorithm follows:
 - quantize the parameter space between appropriate minimum and maximum values of a and b : $a: 1, \dots, K$, $b: 1, \dots, L$
 - store an accumulator array $A(a, b)$ which is initialized to zero dimensions of $A(a, b): K \times L$
 - for each point (x, y) in the thresholded edge image and for each of the desired values of k ($k=1, \dots, K$), calculate b and round it to the nearest discrete value b_k then increment the accumulator $A(a_k, b_k) = A(a_k, b_k) + 1$
 - find maxima in the accumulator array corresponds to collinear points; the value in the accumulator array corresponds to the number of points on the line. The number of lines retained can be set by adjusting a threshold value.
- Amount of calculation: NK (usually $K \ll N$)

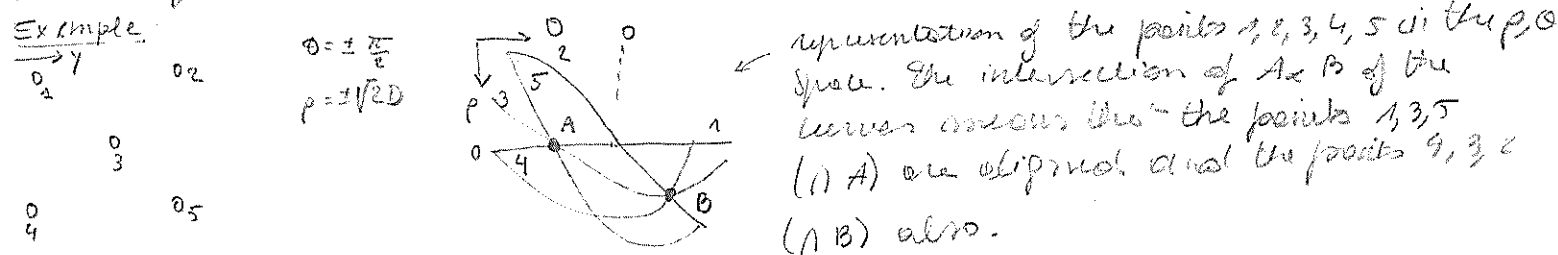


Image Processing

The Wavelet Transform

ADRIAN MUNTEANU

1.1 Vector spaces and Inner Products

Linear Algebra:

- Vectors over R or C that are of a finite dimension n : \mathbb{R}^n or \mathbb{C}^n
- Given $\{v_k\}$ a set of vectors in these spaces:
- Does the set span the spaces, i.e. can every vector be represented as a linear combination of vectors from $\{v_k\}$?
- Are the vectors linearly independent?
- How can we find bases for the spaces to be spanned?
- Given a subspace in \mathbb{R}^n or \mathbb{C}^n and a general vector x , can we find an approximation of x in the least-square sense that lies in the subspace?

Contents

1. Fundamentals of Signal Decompositions
2. Why Wavelets?
3. Time-Frequency Representations
4. CWT, STFT and Frame Theory
5. The Multiresolution Representation
6. Applications
 - Wavelet Based Image Coding
 - Multiscale Edge Detection via CWT
 - Image Enhancement using Wavelets
 - Wavelet based Denoising
7. Wavelet Bases & Filter Banks

1.1 Vector spaces and Inner Products

> A vector space over R or C is a set of vectors E , together with addition and scalar multiplication.

> Properties:

- Commutativity: $x + y = y + x$
- Associativity: $(x + y) + z = x + (y + z)$
- Distributivity: $\alpha(x + y) = \alpha x + \alpha y$
- Additive Identity: there exists 0 in E , such that: $x + 0 = x, \forall x \in E$
- Multiplicative Identity: $1 \cdot x = x, \forall x \in E$
- Additive Inverse: for all x in E , there exists a $(-x)$ in E , such that: $x + (-x) = 0$

> A subset M of E is a subspace of E if:

- For all x and y in M , $x + y$ is in M
- For all x in M , and α in R or C , αx is in M .

> Given $S \subset E$, the span of S is the subspace of E consisting of all linear combinations of vectors in S .

◦ Example:

$$\text{span}(S) = \left\{ \sum_{i=1}^n \alpha_i x_i \mid \forall \alpha_i \in C, \forall x_i \in S \right\}$$

$A \perp E \Leftrightarrow A \oplus E = \mathbb{R}^2$

A is the orthogonal complement of E

$E = \text{span}(x, y) \subset \mathbb{R}^2$

$v = (x_1, y_1, z_1) \in \mathbb{R}^3$

$A \perp E \Leftrightarrow A \oplus E = \mathbb{R}^2$

A is the orthogonal complement of E

$E = \text{span}(x, y) \subset \mathbb{R}^2$

$v = (x_1, y_1, z_1) \in \mathbb{R}^3$

allows to make measurements in a signal

1.1 Vector spaces and Inner Products

- The vectors $\{x_1, x_2, \dots, x_n\}$ are linearly independent if $\sum \alpha_i x_i = 0 \Rightarrow \alpha_i = 0, \forall i$
- A basis in E is a subset of linearly independent vectors $\{x_1, x_2, \dots, x_n\}$ for which: $E = \text{span}(x_1, \dots, x_n)$
- E is infinite dimensional if it contains an infinite linearly independent set of vectors; eg.: the space of infinite sequences is spanned by the infinite set $\{\delta(n-k)\}_{k \in \mathbb{Z}}$
- The inner product on E over \mathbb{C} is a function defined on $E \times E$ with the properties:
 - $\langle x+y, z \rangle = \langle x, z \rangle + \langle y, z \rangle$
 - $\langle x, \alpha y \rangle = \alpha \langle x, y \rangle$
 - $\langle x, y \rangle^* = \langle y, x \rangle$
 - $\langle x, x \rangle \geq 0$ and $\langle x, x \rangle = 0$ if and only if $x = 0$
- Examples:
 - The inner product for complex valued functions over \mathbb{R} : $\langle f, g \rangle = \int_{-\infty}^{\infty} f^*(t)g(t)dt$
 - The inner product for complex valued sequences over \mathbb{Z} : $\langle x, y \rangle = \sum_{n=-\infty}^{\infty} x^*[n]y[n]$
- The norm of a vector is defined as: $\|x\| = \sqrt{\langle x, x \rangle}$

1.1 Vector spaces and Inner Products

- Given a Hilbert space E and a subspace S , the orthogonal complement of S in E , denoted by S^\perp is the set: $\{x \in E, x \perp S\}$
- S is closed if it contains all the limits of sequences of vectors in S .
- Given a vector x in E , there exists a unique y in S and a unique z in S^\perp such that: $x = y + z$.
- Result: $E = S \oplus S^\perp$

Examples of Hilbert spaces

Space of square-summable sequences: $\ell^2(\mathbb{Z})$

inner product: $\langle x, y \rangle = \sum_{n=-\infty}^{\infty} x[n]^* y[n]$

norm: $\|x\| = \sqrt{\langle x, x \rangle} = \sqrt{\sum_{n=-\infty}^{\infty} |x[n]|^2} < \infty \Rightarrow$ finite energy

Space of square-integrable functions: $L^2(\mathbb{R})$

inner product: $\langle f, g \rangle = \int_{-\infty}^{\infty} f(t)^* g(t) dt$

norm: $\|f\| = \sqrt{\langle f, f \rangle} = \sqrt{\int_{-\infty}^{\infty} |f(t)|^2 dt}$

1.1 Vector spaces and Inner Products

- A vector x is said to be orthogonal to a set of vectors $S = \{y_i\}$ if $\langle x, y_i \rangle = 0, \forall i$
- Notation: $x \perp S$
- Two spaces S_1 and S_2 are called to be orthogonal if for $\forall x_i \in S_1, x_j \in S_2$
- Notation: $S_1 \perp S_2$
- A set of vectors $\{x_1, x_2, \dots\}$ is called orthogonal if $\forall i, j, i \neq j, x_i \perp x_j$
- An orthonormal set of vectors is an orthogonal set with unit norm: $\langle x_i, x_j \rangle = \delta[i-j]$
- A vector space equipped with an inner product is called an inner product space.
- A sequence of vectors $\{x_n\}$ in E converges to a vector x in E if: $\|x_n - x\| \rightarrow 0$ as $n \rightarrow \infty$
- A sequence of vectors $\{x_n\}$ is called a Cauchy sequence if: $\|x_n - x_m\| \rightarrow 0$ as $n, m \rightarrow \infty$
- If every Cauchy sequence in E converges to a vector in E , then E is called complete
- A complete inner product space is called a Hilbert space.

↳ Hilbert space with inner product

$$\begin{aligned} \langle x_{2j}, y \rangle &= \langle x_{2j}, \sum_k a_k x_k \rangle \\ &= \sum_k a_k \langle x_{2j}, x_k \rangle \\ &= a_{2j} \end{aligned}$$

1 pair 1 k in product

1.1 Vector spaces and Inner Products

Orthonormal Bases in Hilbert spaces

- $S = \{x_i\}$ form an orthonormal basis in E if $\langle x_i, x_j \rangle = \delta[i-j]$ and $\forall y \in E, \exists a_k$, such that:

$$y = \sum_k a_k x_k \quad a_k = \langle x_k, y \rangle$$

to prove (using def of \perp property of \perp)

Orthogonal Projection and Least-square Approximation

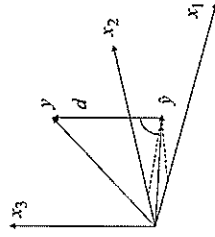
- Given E a Hilbert space, S a closed subspace of E , $\{x_1, x_2, \dots\}$ an orthonormal basis in S , and a vector $y \in E$, find the best approximation of y in S .

$d = y - \hat{y}$

$\|d\| = \|y - \hat{y}\|$ is minimal for $\hat{y} = \sum_i \langle x_i, y \rangle x_i$

Note that: $d \perp S$

Note that: $\|y\|^2 = \|\hat{y}\|^2 + \|d\|^2$



1.1. Vector spaces and Inner Products

Biorthogonal Bases

A system $\{\tilde{x}_k, \tilde{x}_k\}$ constitutes biorthogonal base in a Hilbert space E if and only if:

- For all i, j in \mathbb{Z} : $\langle \tilde{x}_i, \tilde{x}_j \rangle = \delta[i - j]$
- The sets $\{\tilde{x}_k\}$ and $\{\tilde{x}_k\}$ constitute each a frame in E , that is, for all y in E , there exist strictly positive constants (called frame bounds) such that:

$$\|y\|^2 \leq \sum_k |\langle \tilde{x}_k, y \rangle|^2 \leq B \|y\|^2 \rightarrow \text{if } A = B = 1 \rightarrow \text{normalized theorem: energy in original domain} = \text{energy in dual domain} \Rightarrow \text{energy conservation}$$

$$\|\tilde{A}\|y\|^2 \leq \sum_k |\langle \tilde{x}_k, y \rangle|^2 \leq B \|y\|^2 \rightarrow \text{energy of original coefficient should be bounded.}$$
- Bases that satisfy these constraints are called Riesz bases.
- If $A = B$ the frame $\{\tilde{x}_k\}$ is called a tight frame.

Expansion formula: $y = \sum_k \langle \tilde{x}_k, y \rangle \tilde{x}_k = \sum_k \frac{\langle \tilde{x}_k, y \rangle}{\langle \tilde{x}_k, \tilde{x}_k \rangle} \tilde{x}_k$

\Rightarrow reconstruction done in convolution domain of the transform does not have to be the same

10

2.1. Fourier Theory

The signal to be expanded is either continuous or discrete in time.

The expansion involves an integral (a transform) or a summation (a series).

\Rightarrow Four possible combinations of continuous/discrete time and integral/series expansions

General Case

$\{\psi_\omega\}, \{\tilde{\psi}_k\}$ a continuous and a discrete set of basis functions respectively.

(a) Continuous-time Integral Expansion

$$x(t) = \int X_\omega \psi_\omega(t) d\omega, \quad X_\omega = \langle \tilde{\psi}_\omega(t), x(t) \rangle$$

(b) Continuous-time Series Expansion

$$x(t) = \sum_k X_k \psi_k(t), \quad X_k = \langle \tilde{\psi}_k(t), x(t) \rangle$$

(c) Discrete-time Integral Expansion

$$x[n] = \int X_\omega \psi_\omega[n] d\omega, \quad X_\omega = \langle \tilde{\psi}_\omega[n], x[n] \rangle$$

(d) Discrete-time Series Expansion

$$x[n] = \sum_k X_k \psi_k[n], \quad X_k = \langle \tilde{\psi}_k[n], x[n] \rangle$$

11

2. Why Wavelets?

2.1. Review of the Fourier Theory

2.2. Drawbacks of the Fourier Analysis

\Rightarrow energy conservation

2.1. Fourier Theory

Fourier Case

- Continuous-time Fourier Transform (CTFT) - Fourier Transform
- Continuous-time Fourier Series (CTFS) - Fourier Series
- Discrete-time Fourier Transform (DTFT)
- Discrete-time Fourier Series (DTFS)

All cases: $\{\psi\} = \{\tilde{\psi}\}$

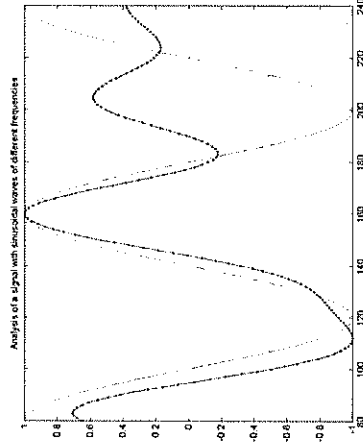
12

2.1.1.1 Fourier Transform

The Fourier Transform in $L^1(\mathbb{R})$

$$\begin{aligned} F(\omega) &= \int_{-\infty}^{\infty} f(t) e^{-j\omega t} dt, \\ \psi_{\omega}(t) &= e^{j\omega t} \quad F(\omega) = \langle e^{j\omega t}, f(t) \rangle \end{aligned} \quad (1)$$

It measures "the intensity" of the oscillations at the frequency ω in $f(t)$



13

2.1.1.1. Fourier Transform

Properties

Linearity, Shifting, Scaling, Differentiation/Integration...

Convolution theorem

$$\begin{aligned} h(t) &= f(t) * g(t) = \int f(\tau)g(t-\tau)d\tau \Rightarrow H(\omega) = F(\omega) \cdot G(\omega) \\ f(t) * g(t) &\leftrightarrow F(\omega) \cdot G(\omega) \\ f(t) \cdot g(t) &\leftrightarrow \frac{1}{2\pi} F(\omega) * G(\omega) \end{aligned}$$

Alternative view of the convolution theorem: the complex exponentials $e^{j\omega t}$ are eigenfunctions of the convolution operator.

$$g(t) * e^{j\omega t} = \int_{-\infty}^{\infty} e^{j\omega(t-\tau)} g(\tau) d\tau = e^{j\omega t} \int_{-\infty}^{\infty} e^{-j\omega\tau} g(\tau) d\tau = G(\omega) e^{j\omega t}$$

Parseval's formula
$$\int_{-\infty}^{\infty} f^*(t)g(t)dt = \frac{1}{2\pi} \int_{-\infty}^{\infty} F^*(\omega)G(\omega)d\omega$$

Energy conservation property
$$\int_{-\infty}^{\infty} |f(t)|^2 dt = \frac{1}{2\pi} \int_{-\infty}^{\infty} |F(\omega)|^2 d\omega$$

15

2.1.1.1. Fourier Transform

The Inverse Fourier Transform in $L^1(\mathbb{R})$

$$\text{If } f \in L^1(\mathbb{R}) \text{ and } F \in L^1(\mathbb{R}) \text{ then: } f(t) = \frac{1}{2\pi} \int_{-\infty}^{\infty} F(\omega) e^{j\omega t} d\omega \quad (2)$$

• Synthesize $f(t)$ as a sum of sinusoidal waves $e^{j\omega t}$ of amplitude $F(\omega)$

Note 1: the inversion formula is exact if f is continuous.

Note 2: the inversion formula is exact if $f(t)$ is defined as $(f(t^+) + f(t^-))/2$ at a point of discontinuity

Fourier Transform in $L^2(\mathbb{R})$

The formulas above hold in the L^2 sense: if $\tilde{f}(t)$ is the result of (1) followed by (2), then:

$$\|f(t) - \tilde{f}(t)\|_2 = 0$$

14

2.1.2. Fourier Series

A periodic signal, $f(t) = f(t + kT)$, $k \in \mathbb{Z}$ can be expanded in its Fourier series:

$$f(t) = \sum_{k=-\infty}^{\infty} F[k] e^{jk\omega_0 t}, \quad \omega_0 = \frac{2\pi}{T}, \quad (3)$$

$$x(t) = \sum_k X_k \psi_k(t) \Rightarrow \psi_k(t) = e^{jk\omega_0 t}$$

• Linear combination of complex exponentials with frequencies $k\omega_0$

Fourier Coefficients:
$$F[k] = \frac{1}{T} \int_{-T/2}^{T/2} f(t) e^{-jk\omega_0 t} dt \quad (4)$$

Note 1: if $f(t)$ is continuous, then the series converges uniformly to $f(t)$

Note 2: if $f(t)$ is square-integrable over a period, but not necessarily continuous, then the series converges to $f(t)$ in L^2 sense.

$$\lim_{N \rightarrow \infty} \|f(t) - \tilde{f}_N(t)\|_2 \rightarrow 0$$

• Convergence plagued by Gibbs phenomenon

16

2.1.2. Fourier Series

Properties

The set of functions used in (3) is a complete orthonormal system for the interval $[-T/2, T/2]$:

$$\varphi_k(t) = (1/\sqrt{T})e^{jk\omega t}, t \in [-T/2, T/2], k \in \mathbb{Z} \Rightarrow \langle \varphi_k(t), \varphi_l(t) \rangle_{[-T/2, T/2]} = \delta[k-l]$$

Parseval relation:

$$\langle g(t), f(t) \rangle = T \cdot \langle F[k], G[k] \rangle \Rightarrow \int_{-T/2}^{T/2} |f(t)|^2 dt = T \cdot \sum_{k=-\infty}^{\infty} |F[k]|^2$$

Best Approximation Property

$$\left\| f(t) - \sum_{k=-N}^N \langle \varphi_k, f \rangle \varphi_k(t) \right\| \leq \left\| f(t) - \sum_{k=-N}^N \alpha_k \varphi_k(t) \right\|, \alpha_k \text{ an arbitrary set of coefficients.}$$

◦ The Fourier series coefficients are the best ones for an approximation in the span of $\{\varphi_k(t)\}, k \in [-N, N]$

Fourier series can be used for non-periodic signals via periodization.

Problem: discontinuities at the boundaries.

17

2.1.3. Discrete-Time Fourier Transform

Properties

The properties of the FT are carried over by DTFT

Convolution:

$$f[n] * g[n] = \sum_{l=-\infty}^{\infty} f[n-l]g[l] = \sum_{l=-\infty}^{\infty} f[l]g[n-l] \leftrightarrow F(e^{j\omega}) \cdot G(e^{j\omega})$$

Parseval's relation:

$$\sum_{n=-\infty}^{\infty} f^*[n]g[n] = \frac{1}{2\pi} \int_{-\pi}^{\pi} F^*(e^{j\omega})G(e^{j\omega})d\omega$$

Energy conservation:

$$\sum_{n=-\infty}^{\infty} |f[n]|^2 = \frac{1}{2\pi} \int_{-\pi}^{\pi} |F(e^{j\omega})|^2 d\omega$$

19

2.1.3. Discrete-Time Fourier Transform

Given a sequence $\{f[n]\}_{n \in \mathbb{Z}}$ in $\ell^2(\mathbb{Z})$, its discrete-time Fourier transform is defined by

$$F(e^{j\omega}) = \sum_{n=-\infty}^{\infty} f[n]e^{-j\omega n}, \text{ which is } 2\pi \text{ periodic.} \quad (5)$$

Inverse transform:

$$f[n] = \frac{1}{2\pi} \int_{-\pi}^{\pi} F(e^{j\omega})e^{j\omega n} d\omega \quad (6)$$

$$x[n] = \int X_{\omega} \psi_{\omega}[n] d\omega \Rightarrow \psi_{\omega}[n] = e^{j\omega n}$$

Note 1: If $f[n]$ is in $\ell^2(\mathbb{Z})$, we have convergence in ℓ^2 sense as the summation limits in (5) go to infinity.

Note 2: $f[n]$ is obtained by sampling a continuous time signal $f(t)$ at instants nT .

Result: DTFT is related to the Fourier transform $F_c(\omega)$ of $f(t)$:

$$F(e^{j\omega}) = \frac{1}{T} \sum_{k=-\infty}^{\infty} F_c\left(\omega - k\frac{2\pi}{T}\right)$$

19

2.1.4. Discrete-Time Fourier Series

A periodic discrete signal, $f[n] = f[n+IN], I \in \mathbb{Z}$ has its discrete-time Fourier series representation given by:

$$F[k] = \sum_{n=0}^{N-1} f[n]e^{-jn k 2\pi/N}, \quad k \in \mathbb{Z} \quad (7)$$

$$\text{Inverse DTFS representation: } f[n] = \frac{1}{N} \sum_{k=0}^{N-1} F[k]e^{jn k 2\pi/N}, \quad n \in \mathbb{Z} \quad (8)$$

$$x[n] = \sum_k X_k \psi_k[n] \Rightarrow \psi_k[n] = e^{jn k 2\pi/N}$$

All the properties of the FT hold.

Convolution \Rightarrow Circular Convolution

$$\Rightarrow f_0[n], g_0[n], \text{ one period of } f[n], g[n]$$

$$\Rightarrow f_0[n] = \begin{cases} f[n], & 0 \leq n \leq N-1 \\ 0, & \text{otherwise} \end{cases}$$

20

2.1.4. Discrete-Time Fourier Series

Circular Convolution

$$\begin{aligned} f[n] \circ g[n] &= \sum_{l=0}^{N-1} f[n-l]g[l] = \sum_{l=0}^{N-1} f_0[(n-l) \bmod N]g_0[l] = \\ &= f_0[n] \circ g_0[n] \end{aligned}$$

Parseval's relation:

$$\sum_{n=0}^{N-1} f^*[n]g[n] = \frac{1}{N} \sum_{k=0}^{N-1} F^*[k]G[k]$$

Discrete Fourier Transform (DFT)

The same formulas as (7) and (8), except that $f[n]$ and $F[k]$ are defined only for: $n, k \in \{0, \dots, N-1\}$

Convolution matrix C:

$$C = \begin{pmatrix} f[0] & f[1] & \dots & f[N-1] \\ f[N-1] & f[0] & \dots & f[N-2] \\ \vdots & \vdots & \ddots & \vdots \\ f[1] & f[2] & \dots & f[0] \end{pmatrix}$$

2.1.4. Discrete-Time Fourier Series

Circular Convolution

$$f \circ g = Cg = F^{-1} \Lambda F g, \quad F[n][k] = e^{-jnk2\pi/N}, \quad F^{-1}[n][k] = (1/N)e^{jn k 2\pi/N}$$

Λ is a diagonal matrix with $F[k]$ on its diagonal.

Another view:

• C is diagonalized by F

• The complex exponential sequences $\{e^{j(2\pi/N)nk}\}$ are eigenvectors for the convolution matrix C, with eigenvalues $F[k]$.

$$\hat{f} = Ff, \quad \hat{g} = Fg$$

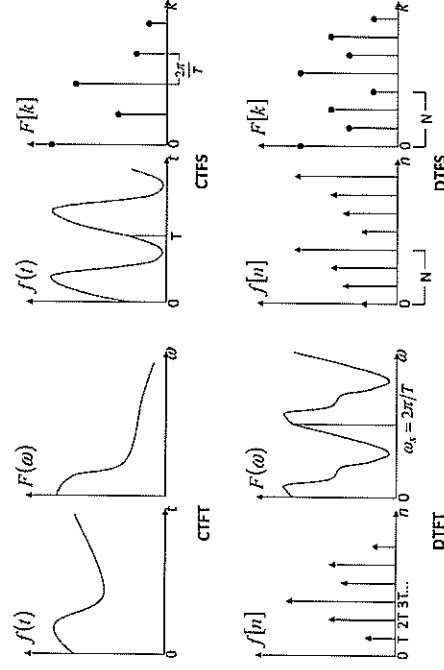
Parseval's relation:

$$\hat{f}^* \hat{g} = (Ff)^* (Fg) = f^* F^* F g = N f^* g; \quad F^{-1} = \frac{1}{N} F^*$$

2.1.5 Various Flavors of Fourier Transforms

Transform	Time	Frequency	Analysis Synthesis
Fourier Transform CTFT	Continuous	Continuous	$F(\omega) = \int_{-\infty}^{\infty} f(t) e^{-j\omega t} dt$ $f(t) = 1/2\pi \int_{-\infty}^{\infty} F(\omega) e^{j\omega t} d\omega$
Fourier Series CTFS	Continuous Periodic	Discrete	$F[k] = 1/T \int_{-T/2}^{T/2} f(t) e^{-j2\pi k t/T} dt$ $f(t) = \sum_k F[k] e^{j2\pi k t/T}$
Discrete-Time Fourier Transform DTFT	Discrete	Continuous Periodic	$F(e^{j\omega}) = \sum_{n=-\infty}^{\infty} f[n] e^{-j\omega n}$ $f[n] = 1/2\pi \int_{-\pi}^{\pi} F(e^{j\omega}) e^{j\omega n} d\omega$
Discrete-Time Fourier Series DTFS	Discrete Periodic	Discrete Periodic	$F[k] = \sum_{n=0}^{N-1} f[n] e^{-j2\pi k n/N}$ $f[n] = 1/N \sum_{k=0}^{N-1} F[k] e^{j2\pi k n/N}$

2.1.5 Various Flavors of Fourier Transforms



CASE: PARAMETRIC CURVES

7

In this case, the goal is, given n points in an image, find all sets of these points that lie on curves $c(x, y, p_1, \dots, p_N) = 0$ parameters p_i . The dimension of the p, θ space depends on the number of parameters (of the order) of the curve. The higher the order, the higher the dimension of the accumulator.

The algorithm is similar but the 3rd step has to be modified because there is an exponential growth of the calculations and of the size of the accumulator with the number of parameters. To save computation in the accumulator, gradient orientation information is used.

EX: a 3 parameter curve $(a, b, r): (x-a)^2 + (y-b)^2 = r^2$: for each distinct value of r , restrict the range and quantization steps of the x and y centers.

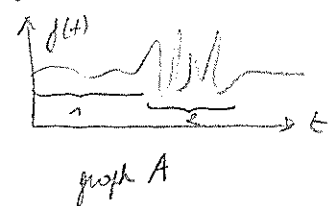
CHAPTER 3: WAVELET TRANSFORM

FUNDAMENTALS OF SIGNAL DECOMPOSITION (from slide 1-24: not for exam, only read)

my notes - part 4x4 slide 22-25

INTRODUCTION TO WAVELET TRANSFORM

The Fourier transform expresses a signal from exponentials, extracting the frequency component of the function in time $f(t)$. The problem is that, if this gives a very nice frequency localization of the signal (Dirac pulses at right frequency), the localization in time is almost none of the analysis from $-\infty$ to $+\infty$ of the signal. The peak of the wavelet transform is thus to localize the analysis the localized basis function in time and frequency by capturing signal transform. For example:



one part 1 of the signal should have a different frequency content than part 2, thus it be separated into different analysis rather than 1 fit on the whole signal such as Fourier.

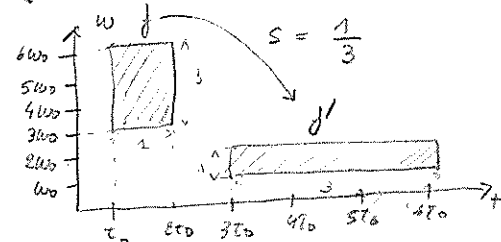
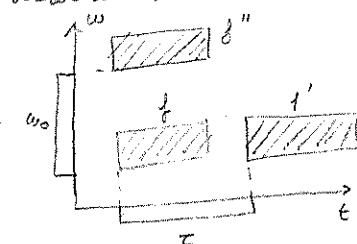
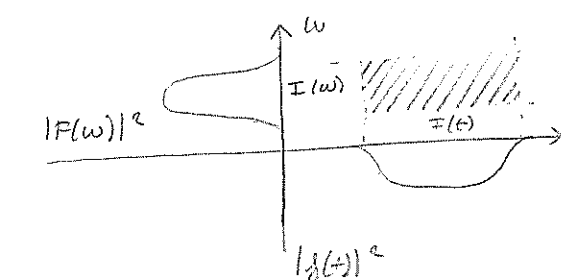
$$F(\omega) = \int_{-\infty}^{+\infty} f(t) e^{-j\omega t} dt$$

time interval extraction in frequency

TIME-FREQUENCY REPRESENTATION

A tile is defined in the time-frequency plane as containing 90% of the energy of the time and frequency domain functions. It is centered around the centers of gravity of $|f(t)|^2$ and $|F(\omega)|^2$. The basis function defined by it is of finite local in time and frequency. Its properties are:

- time shift $\tau \rightarrow$ shifting of the tile by τ in time axis
- modulation by $e^{j\omega_0 t} \rightarrow$ shifting of the tile by ω_0 in frequency axis
- scaling by s ($f'(t) = f(st)$) $\rightarrow I'_t = \frac{I_t}{s}$ and $I'_\omega = s I_\omega$ i.e resolution in frequency is resolved for resolution in time



Demo:

Time support of $f(t)$: $I_t = [-T, +T]$

By defining $f'(t) = f(st)$, $s > 0$ we have

$-T \leq t \leq T \Rightarrow -T \leq st \leq T \Rightarrow -\frac{T}{s} \leq t \leq \frac{T}{s}$ then

Time support of $f'(t)$: $I'_t = \frac{I_t}{s}$

Frequency support of $f(t)$: $I_\omega = [\omega_{min}, \omega_{max}]$
By defining $F'(\omega) = \int_{-T/s}^{T/s} f'(t) e^{-j\omega t} dt = \int_{-T}^{T} f(st) e^{-j\omega t} dt$

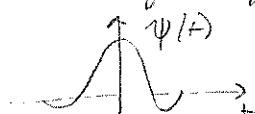
change $st \rightarrow t'$
 $= \frac{1}{s} \int_{-T}^{T} f(t') e^{-j(\frac{\omega}{s})t'} dt' = \frac{1}{s} F(\frac{\omega}{s})$

$\omega_{min} \leq \omega \leq \omega_{max}$, $\omega_{min} \leq \omega' = \frac{\omega}{s} \leq \omega_{max}$

$\Rightarrow s \omega_{min} \leq \omega \leq s \omega_{max}$
frequency support of $f'(t)$ is $I'_\omega = s I_\omega$

The basis functions used for the wavelet transform uses these properties. They are defined as:

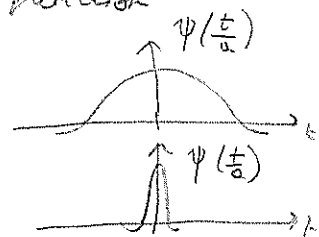
$\psi_{a,b}(t) = \frac{1}{\sqrt{a}} \psi\left(\frac{t-b}{a}\right)$ and transform $\langle f(t), \psi_{a,b}(t) \rangle$



1. Scaling by a

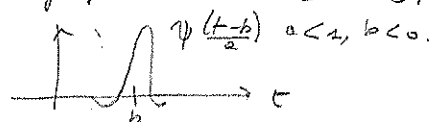
The notion of scale is similar to that used in geographical maps
 The scale can also be seen as a frequency analysis in the case where the wave function acts as a band-pass filter
 large scale = global view
 small scale = detailed view
 large scale = low frequency band function
 small scale = high frequency band function
 Thus the scale is directly related to the inverse frequency.

→ large scale: $a > 1$, $\psi_{a,b}(t)$ identifies long term trend in $f(t)$
 → small scale: $a < 1$, $\psi_{a,b}(t)$ identifies short term behavior in $f(t)$



2. Shifting by b

It allows to move the wave function in time



3. Normalization factor

This factor ensures that the scaled ψ_a has the same energy as the original ψ

$$\int |\psi(t)|^2 dt = \int \psi(t) \psi^*(t) dt$$

$$\int |\psi_{a,b}(t)|^2 dt = \int \frac{1}{\sqrt{a}} \psi\left(\frac{t}{a}\right) \cdot \frac{1}{\sqrt{a}} \psi^*\left(\frac{t}{a}\right) dt = \int \psi(t') \psi^*(t') dt' = \int |\psi(t)|^2 dt \quad \text{if } a = 1$$

The limit cannot be made arbitrarily as small as possible to have sharp analysis both in time and in frequency simultaneously. The uncertainty principle defines the limitation on the width and length of the wave. It is defined as

$$\Delta t^2 \cdot \Delta \omega^2 \geq \frac{1}{4} \quad \text{where} \quad \Delta t^2 = \frac{\int t^2 |\psi(t)|^2 dt}{\int |\psi(t)|^2 dt} \quad \text{is the resolution in time}$$

$$\Delta \omega^2 = \frac{\int \omega^2 |\psi(\omega)|^2 d\omega}{\int |\psi(\omega)|^2 d\omega} \quad \text{is the resolution in frequency}$$

$\psi(t)$ is a wave function with Fourier transform $\psi(\omega)$
 centered around origin in time & frequency respectively.
 $\int |\psi(t)|^2 dt = 0$ and $\int \omega |\psi(\omega)|^2 d\omega = 0$

Equality holds for Gaussian functions, $\psi(t) = \sqrt{\frac{2\alpha}{\pi}} e^{-\alpha t^2}$

Demo: $\Delta t^2 \cdot \Delta \omega^2 \geq \frac{1}{4} \Leftrightarrow \left(\int_{-\infty}^{+\infty} t^2 |\psi(t)|^2 dt \right) \left(\int_{-\infty}^{+\infty} \omega^2 |\psi(\omega)|^2 d\omega \right) \geq \frac{1}{4} \left(\int_{-\infty}^{+\infty} |\psi(t)|^2 dt \right) \left(\int_{-\infty}^{+\infty} |\psi(\omega)|^2 d\omega \right)$

By Parseval's formula: $\int_{-\infty}^{+\infty} |\psi(t)|^2 dt = \frac{1}{2\pi} \int_{-\infty}^{+\infty} |\psi(\omega)|^2 d\omega$

$$\geq \frac{\pi}{2} \left(\int_{-\infty}^{+\infty} |\psi(t)|^2 dt \right)^2$$

By $\psi'(t) \rightarrow j\omega \psi(\omega)$ and $\psi'(t)^* \rightarrow -j\omega \psi^*(\omega)$ and Parseval: $\int_{-\infty}^{+\infty} |\psi'(t)|^2 dt = \frac{1}{2\pi} \int_{-\infty}^{+\infty} \omega^2 |\psi(\omega)|^2 d\omega$

$$\Leftrightarrow \left(\int_{-\infty}^{+\infty} t^2 |\psi(t)|^2 dt \right) \left(\int_{-\infty}^{+\infty} |\psi'(t)|^2 dt \right) \geq \frac{1}{4} \left(\int_{-\infty}^{+\infty} |\psi(t)|^2 dt \right)^2$$

By Cauchy-Schwarz inequality: $\left(\int_{-\infty}^{+\infty} f(t) g(t) dt \right)^2 \leq \left(\int_{-\infty}^{+\infty} f(t)^2 dt \right) \left(\int_{-\infty}^{+\infty} g(t)^2 dt \right)$

By replacing the variables: $f(t) = t \psi(t)$ and $g(t) = \psi'(t)$

$$\Leftrightarrow \left(\int_{-\infty}^{+\infty} t^2 |\psi(t)|^2 dt \right) \left(\int_{-\infty}^{+\infty} |\psi'(t)|^2 dt \right) \geq \left| \int_{-\infty}^{+\infty} t \psi(t) \psi'(t) dt \right|^2 =: I^2$$

thus $I = \int_{-\infty}^{+\infty} t \psi(t) \psi'(t) dt = t \psi^2(t) \Big|_{-\infty}^{+\infty} - \int_{-\infty}^{+\infty} (\psi(t) + t \psi'(t)) \psi(t) dt = 0 - \int_{-\infty}^{+\infty} \psi^2(t) dt - I$
 (integrate by parts)

$$\pm = \frac{1}{2} \int_{-\infty}^{\infty} \psi^2(t) dt \Rightarrow \pm^2 = \frac{1}{4} \left(\int_{-\infty}^{\infty} \psi^2(t) dt \right)^2$$

the equality holds for: $\psi'(t) = k \pm \psi(t)$
 $k = -2\alpha$
 $\int_{-\infty}^{\infty} \psi^2(t) dt = 1$
 $\Rightarrow \psi(t) = \sqrt{\frac{2\alpha}{\pi}} e^{-\alpha t^2}$

CONTINUOUS SHORT-TIME FOURIER TRANSFORM

the goal is to improve the localization properties of the Fourier transform

continuous transform: $STFT_f(\tau, \omega) = \int_{-\infty}^{\infty} f(t) w^*(t - \tau) e^{-j\omega t} dt$ window time shift
 $= \langle g_{\omega, \tau}(t), f(t) \rangle$ where $g_{\omega, \tau}(t) = \overbrace{w(t - \tau)}^{\uparrow} e^{j\omega t}$
 is the windowed complex exponential.

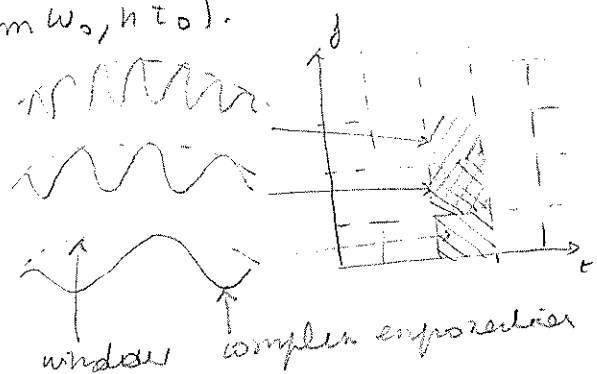
It is the inner product between the signal and the "shifts and modulates of our elementary window"

inverse transform: $f(t) = \frac{1}{2\pi \|w(t)\|^2} \int_{-\infty}^{\infty} \int_{-\infty}^{\infty} STFT_f(\omega, \tau) g_{\omega, \tau}(t) d\omega d\tau$
 superposition of functions in transform domain

Any choice window used for Fourier analysis is suitable for STFT transform. smooth window are preferred (e.g. Hanning window $w(t) = \begin{cases} [1 + \cos(2\pi t/T)]/2 & t \in [-T/2, T/2] \\ 0 & \text{else} \end{cases}$). It is also convenient to choose the window such that $\|w(t)\| = \|w(t)\|_2^2 = 1$, i.e. normalized window. Gaussian window (e.g. Gabor: $w(t) = e^{-\alpha t^2}$, $\alpha > 0$) with α controlling the width and p normalization factor) allows to reach equality in the uncertainty principle.

The Parseval's formula is written as: $\int_{-\infty}^{\infty} |f(t)|^2 dt = \frac{1}{2\pi} \int_{-\infty}^{\infty} \int_{-\infty}^{\infty} |STFT_f(\omega, \tau)|^2 d\omega d\tau$

and as the time-frequency resolution of each elementary function is constant, it is natural to discretize the STFT on a rectangular grid $(m\omega_0, n\tau_0)$.

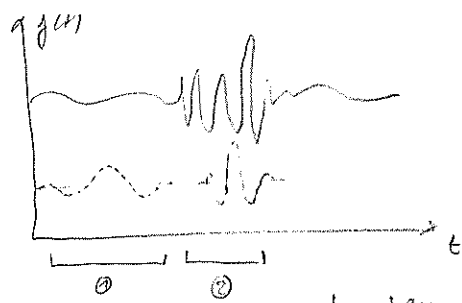


once the window size is chosen, all frequencies are analyzed with the same time and frequency resolution, unlike what happens in the Wavelet Transform. It is not possible to distinguish different behaviors within a window spread. The alternative is to use a generalized STFT with multiple window sizes but this implies overcomplete representations (to much info)

CONTINUOUS WAVELET TRANSFORM

The drawback introduced by the STFT is the constant resolution in time and frequency. To overcome this, the wavelet transform supposes the equality in the Heisenberg principle (uncertainty principle): $\Delta t \cdot \Delta \omega = \frac{1}{2}$ which holds

constant relative bandwidth analyzed: $\frac{\Delta f}{f} = cte \Rightarrow \Delta f = c \cdot f \cdot \Delta \omega = 2\pi \Delta f \Rightarrow$
 $\Delta t \cdot 2\pi c f = \frac{1}{2} \Rightarrow \Delta t = \frac{1}{4\pi c \cdot f}$ thus $\begin{cases} HF \Rightarrow f \uparrow \Delta t \downarrow \text{ (good localization in frequency)} \\ LF \Rightarrow f \downarrow \Delta t \uparrow \text{ (good localization in time)} \end{cases}$



- ① good localization in frequency: distance between closed low-frequency curves, the transform is able to discriminate the neighboring frequencies
- ② good localization in time: distance between closed spikes in time

The transform can be seen as a real band-pass filter with impulse response $\psi(t)$, zero mean, $\int_{-\infty}^{+\infty} \psi(t) dt = 0$ and unit energy.

forward transform: $CWT_f(a, \tau) = \frac{1}{\sqrt{a}} \int_{-\infty}^{+\infty} f(t) \psi^*\left(\frac{t-\tau}{a}\right) dt$ for $f(t) \in L^2(\mathbb{R})$

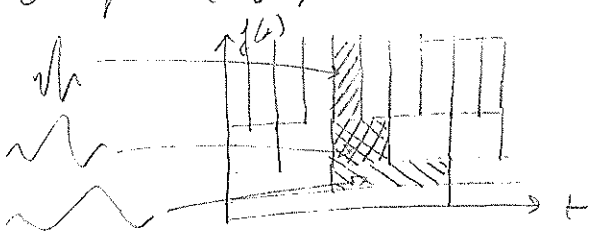
The CWT measures the similarity between the signal and the scaled and shifted version of the elementary wave function $\psi_{a,\tau}(t) = \frac{1}{\sqrt{a}} \psi\left(\frac{t-\tau}{a}\right)$

Inverse transform: if the wavelet $\psi(t)$ satisfies the admissibility condition

$CWT_f(a, \tau) = \langle f(t), \psi_{a,\tau}(t) \rangle$ with $\Psi(\omega)$ the Fourier transform of $\psi(t)$,
 $C_\psi = \int_{-\infty}^{+\infty} \frac{|\Psi(\omega)|^2}{|\omega|^3} d\omega < \infty$ (imposes that $|\Psi(\omega)|^2$ goes down faster than ω^2 , and too demanding)

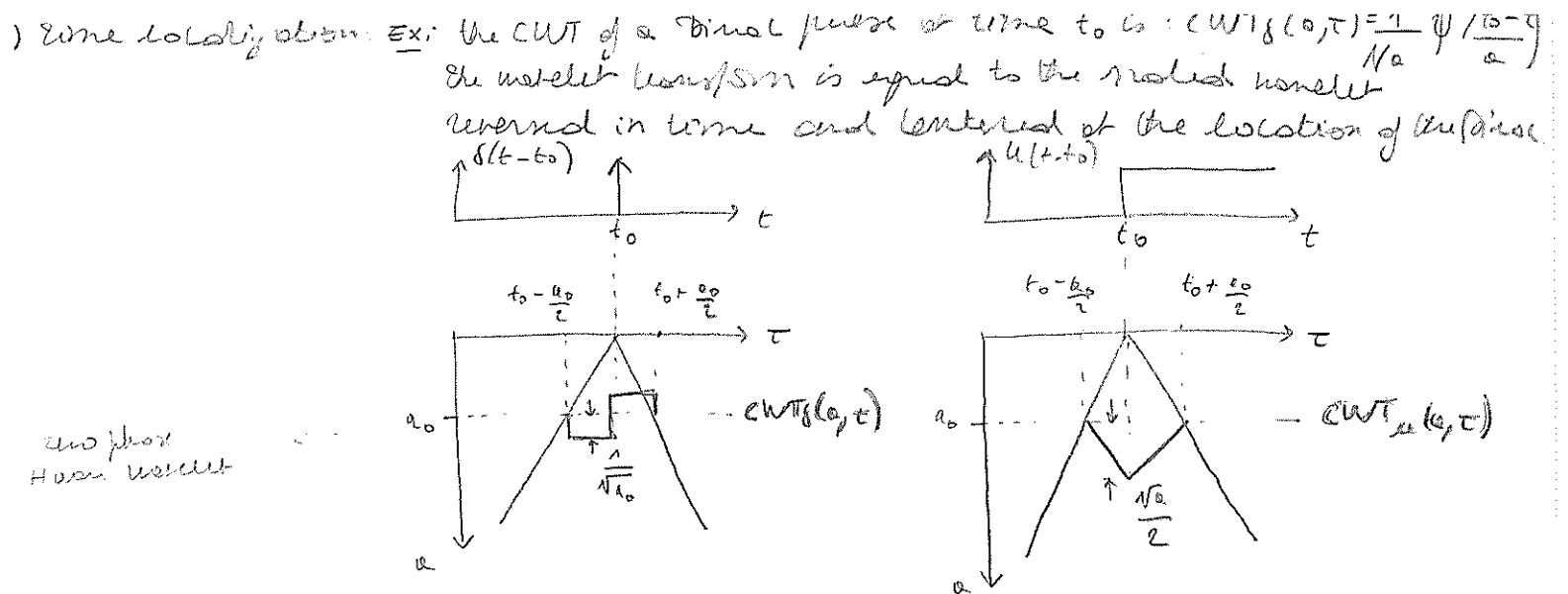
$f(t) = \frac{1}{C_\psi} \int_{-\infty}^{+\infty} \int_{-\infty}^{+\infty} CWT_f(a, \tau) \psi_{a,\tau}(t) \frac{da d\tau}{a^2}$

Any $f(t) \in L^2(\mathbb{R})$ can be written as a superposition of shifted and dilated wavelets. The reconstruction is in the L^2 sense (the L^2 norm of the reconstruction error is 0). The distribution of time-frequency space uses large time steps for large a ($a > 1$) as in this case, $\psi_{a,\tau}(t)$ is "long" and of low frequency and fine time steps for small a ($a < 1$) as in this case $\psi_{a,\tau}(t)$ is "short" and of high frequency. This defines the tiling of the frequency-time plane (a, τ) in the form (a_0^n, τ_0^n) .



Properties

- ① linearity: follows from the linearity of the inner product
- ② shift property: if $g(t) = f(t - \tau')$ $\Rightarrow CWT_g(a, \tau) = CWT_f(a, \tau - \tau')$, $t' = t - \tau'$
 Proof: $CWT_g(a, \tau) = \frac{1}{\sqrt{a}} \int_{-\infty}^{+\infty} f(t - \tau') \psi^*\left(\frac{t - \tau}{a}\right) dt = \frac{1}{\sqrt{a}} \int_{-\infty}^{+\infty} f(t') \psi^*\left(\frac{t' + \tau - \tau}{a}\right) dt'$
 $u = t - \tau'$
 $du = dt$
 $= \frac{1}{\sqrt{a}} \int_{-\infty}^{+\infty} f(t') \psi^*\left(\frac{t' - (\tau - \tau')}{a}\right) dt'$, comme $u = t - \tau' \Rightarrow \tau = \tau - \tau'$
 $= CWT_f(a, \tau - \tau')$
- ③ Scaling property: if $g(t) = \frac{1}{\sqrt{b}} f\left(\frac{t}{b}\right) \Rightarrow CWT_g(a, \tau) = CWT_f\left(\frac{a}{b}, \frac{\tau}{b}\right)$
 Proof: $CWT_g(a, \tau) = \frac{1}{\sqrt{a}} \int_{-\infty}^{+\infty} \frac{1}{\sqrt{b}} f\left(\frac{t}{b}\right) \psi^*\left(\frac{t - \tau}{a}\right) dt = \frac{1}{\sqrt{a}} \int_{-\infty}^{+\infty} \frac{1}{\sqrt{b}} f(t') \psi^*\left(\frac{bt' - \tau}{a}\right) dt' \xrightarrow{t' = \frac{t}{b}} \frac{1}{\sqrt{a}} \int_{-\infty}^{+\infty} \frac{1}{\sqrt{b}} f(t') \psi^*\left(\frac{bt' - \tau}{a}\right) dt' \xrightarrow{t' = \frac{t}{b}} \frac{1}{\sqrt{a}} \int_{-\infty}^{+\infty} \frac{1}{\sqrt{b}} f(t') \psi^*\left(\frac{t' - \frac{\tau}{b}}{a/b}\right) dt' = CWT_f\left(\frac{a}{b}, \frac{\tau}{b}\right)$



Two plots:
Horn wavelet

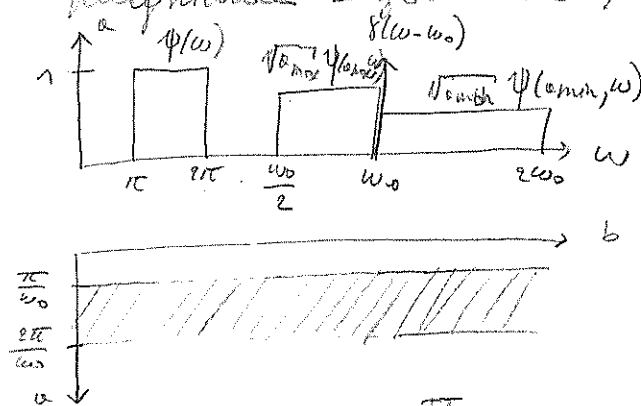
The transform "zooms-in" to the Dirac or into the step function with a very good localization for very small scales a

Proof: the horn wavelet transform is $\psi(t) = \begin{cases} 1 & 0 \leq t \leq \frac{1}{2} \\ -1 & \frac{1}{2} \leq t \leq 1 \\ 0 & \text{else} \end{cases}$

Horn it from a triangle into $u(t)$ as a sum of rectangles (etc) gives a triangle (etc)
The line is first 1/2 because of positive part of Horn wavelet combined with a then
obviously because of negative part of Horn wavelet.

+ demo on page applet \rightarrow doi 1558816731771317 pg 4

Frequency localization: ex: A complex sinusoid of unit magnitude at frequency ω_0
The "min wavelet" (a perfect bandpass filter) with
magnitude 1 for $\omega \in [\omega_0 - \pi, \omega_0 + \pi]$



The highest frequency
wavelet that can analyze
the signal has a scale
 $a_{min} = \frac{\pi}{\omega_0}$ and the
lowest frequency wavelet
that can analyze the
signal has the scale
 $a_{max} = \frac{9\pi}{\omega_0}$ hence:

$$\psi(t) \xrightarrow{FT} \Phi(\omega) \Rightarrow \left\{ \begin{aligned} \psi\left(\frac{t}{a}\right) &\xrightarrow{FT} a \Phi(a\omega) \text{ scaling} \\ \frac{1}{\sqrt{a}} \psi\left(\frac{t}{a}\right) &\xrightarrow{FT} \sqrt{a} \Phi(a\omega) \text{ energy} \end{aligned} \right.$$

Thus: $a\omega_0 = \omega$ and $\omega = 2\pi \Rightarrow a = \frac{2\pi}{\omega_0}$ hence the lowest
freq. wavelet which can still analyze the signal is $a = a_{min}$
 $a\omega_0 = \omega$ and $\omega = \pi \Rightarrow a = \frac{\pi}{\omega_0}$ hence the highest
freq. wavelet which can still analyze the signal is $a = a_{max}$

Proof: demo on page applet \rightarrow idem u-leson

The frames of the WT and the STFT are means to discretize these continuous-time transforms to represent the signal via set of transform coefficient and reconstruct the signal in a stable way:

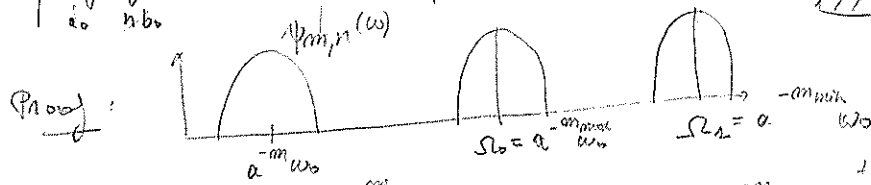
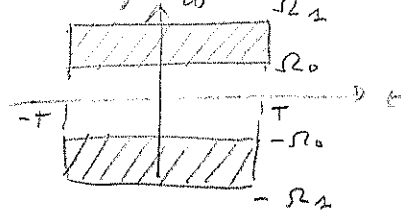
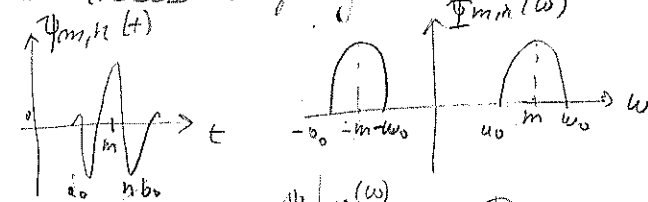
$$g_{\omega, \tau} \xrightarrow{\text{discretize } \omega, \tau} g_{m, n} \text{ such that } f = \sum_m \sum_n \langle g_{m, n}, f \rangle \tilde{g}_{m, n}$$

$$\psi_{\omega, \tau} \xrightarrow{\text{discretize } \omega, \tau} \psi_{m, n} \text{ such that } f = \sum_m \sum_n \langle \psi_{m, n}, f \rangle \tilde{\psi}_{m, n}$$

Some results done slides 56-58, only to be known for advanced questions at exam \rightarrow to print + add comments.

CWT

Assume that $|\psi|$ and $|\tilde{\psi}|$ are symmetric and centered about $t=0$ and $\omega=\omega_0$ respectively. Then $\psi_{m, n}$ is centered around $t = e_0^m n b_0$ and $\tilde{\psi}_{m, n}$ is centered around $f = \pm e_0^{-m} \omega_0$. $\langle \psi_{m, n}, f \rangle$ is the "information content" of $f(t)$ near $t = e_0^m n b_0$ and $\omega = \pm e_0^{-m} \omega_0$. Assume $f(t)$ is localized in time and frequency, then only the coefficients $\langle \psi_{m, n}, f \rangle$ for which $(t, \omega) = (e_0^m n b_0, e_0^{-m} \omega_0)$ lies within (or very close to) $[-T, T] \times [-\Omega_2, -\Omega_0] \cup [\Omega_0, \Omega_2]$ are needed for f to be reconstructed up to a good approximation.



$$\log_{e_0} \Omega_0 = \log_{e_0} e_0^{-m} \omega_0 \Rightarrow m_{\min} = \log_{e_0} \left(\frac{\omega_0}{\Omega_0} \right)$$

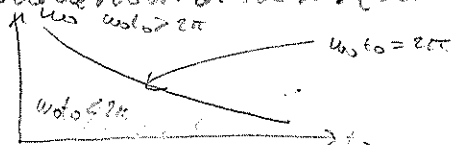
$$\log_{e_0} \Omega_2 = \log_{e_0} e_0^{-m} \omega_0 \Rightarrow m_{\max} = \log_{e_0} \left(\frac{\omega_0}{\Omega_2} \right)$$

$$\Rightarrow \text{comes on limit} \rightarrow a^{-m} \omega_0 \text{ at limits } \psi(\omega) \text{ at limits}$$

STFT

If $g_{m, n}(t)$ constitutes a frame $L^2(\mathbb{R})$ with frame bounds A and B , then $A \leq \frac{2\pi}{\omega_0 b_0} \|g\|^2 \leq B$ (g is missing in this expression \rightarrow no admissibility condition for honest frames ??). Tight frames (for $\|g\|=1$ so g can always be normalized) are defined as $A=B=\frac{2\pi}{\omega_0 b_0}$. ω_0 and b_0 cannot be arbitrarily chosen:

\rightarrow no frames exists for $\omega_0 b_0 > 2\pi$??
 \rightarrow good tight frames for $\omega_0 b_0 \leq 2\pi$ with good time-freq. localization properties but oversampling, with $A=B=\frac{2\pi}{\omega_0 b_0}$ (the oversampling ratio ??)
 \rightarrow orthonormal bases (critical sampling) for $A=B=1 \rightarrow \omega_0 b_0 = 2\pi$ does hold in time-freq



there is no way to construct STFT orthonormal bases with good time-frequency localization. This comes from the Poisson-Ross theorem:

If $\{g_{m,n}(t) = e^{j2\pi m t} w(t-n) \mid m, n \in \mathbb{Z}\}$ constitutes a frame for $L^2(\mathbb{R})$ then either $\int_{\mathbb{R}} |w(t)|^2 dt = \infty$ or $\int_{\mathbb{R}} |w(\omega)|^2 d\omega = \infty$ (setting $\omega_0 = 2\pi$, $t_0 = 1 \Rightarrow \omega_0 t_0 = 2\pi$)

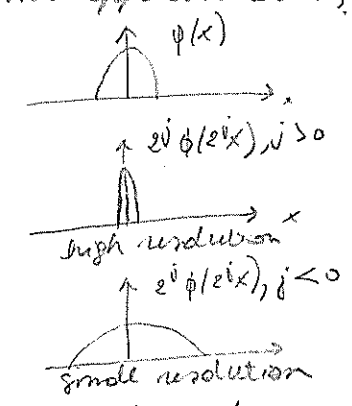
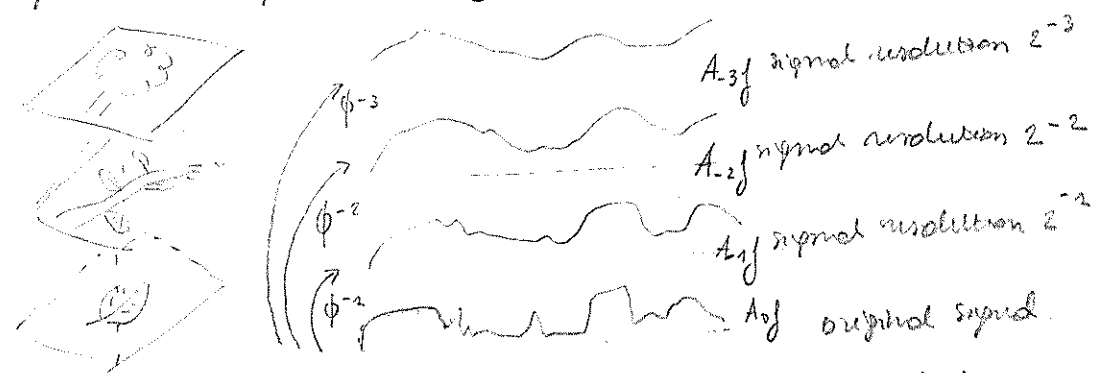
$\Rightarrow g_{m,n}(t) = e^{j2\pi m t} w(t-n t_0)$ with gaussian window $w(t) = \pi^{-1/4} e^{-t^2/2}$

$\tilde{g}_{m,n}(t) = e^{j2\pi m t} \tilde{w}(t-n t_0)$ the dual frame and the window $\tilde{w}(t)$ can be calculated with our iteration procedure for different choices of $\omega_0 = t_0 = (2\pi\lambda)^{1/2}$. \tilde{w} becomes less and less smooth as λ increases (oversampling decreases). For $\lambda < 1$, these frames have good time-frequency localization. For $\lambda = 1$, \tilde{w} is not even square-integrable anymore. Thus there is no STFT orthonormal basis with good time-frequency localization (orthogonal bases are necessarily uniformly sampled). If modulation by cosines is used (instead of modulation by complex exponentials, good orthonormal bases do exist \rightarrow local cosine bases).

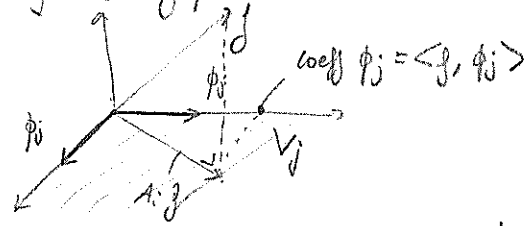
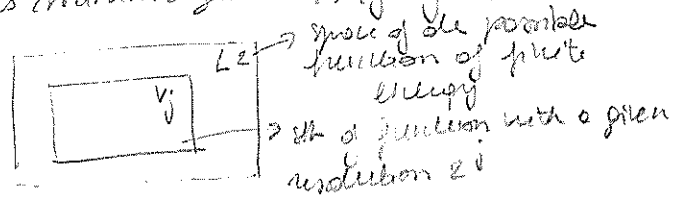
ULTRARESOLUTION REPRESENTATION

scaling functions

The goal is to represent any continuous image as a set of hierarchical approximations.



The scaling functions $\phi_j(x)$, $j < 0$ define the signal resolution and are all derived from one scaling function $\phi(x)$, forming a set of basis: $\phi_j(x) = 2^j \phi(2^j x)$, $j < 0$. The goal is to make an approximation of the signal such that the L^2 norm error is minimized: $\|A_j f - f\|_2$ where $A_j f \in V_j =$ set of possible function at a given resolution 2^j .



$$A_j f(x) = 2^{-j} \sum_{n=-\infty}^{+\infty} \langle f(u), \phi_j(u - 2^{-j}n) \rangle \phi_j(x - 2^{-j}n)$$

$\Rightarrow A_j f$ is the projection of f onto the basis ϕ_j , $\langle f, g \rangle$ is the inner product:
 $\langle f, g \rangle = \int_{-\infty}^{+\infty} f(u) \cdot g(u) du$

$\frac{S}{b} = \sum_{n=-\infty}^{+\infty} \text{coeff}(n) b(n)$
 $\frac{S}{b} = \text{coeff} \frac{b}{b}$

scaling functions is a low pass filter. The set of inner products $A_j^d f(n) = \langle f(u), \phi_j(u - 2^{-j}n) \rangle_{n \in \mathbb{Z}}$ are called the discrete approximation of $f(x)$ at the resolution 2^j . They can be rewritten as $A_j^d f(n) = \langle f(u), \phi_j(u - 2^{-j}n) \rangle = \int_{-\infty}^{+\infty} f(u) \phi_j(u - 2^{-j}n) du = (f(u) * \phi_j(-u))(2^{-j}n)_{n \in \mathbb{Z}}$ which shows that is obtain the discrete approximations

if $A_j f$, f is convolved with a low pass filter and the result is evaluated at $2^{-j}m$ (uniform sampling rate 2^j). In practice $A_j^d f$ are used instead of $A_j f$.

The discrete approximation allows to compact the information in discrete coefficients. The fast algorithm for calculating $A_j^d f$ is called the pyramid algorithm and allows to calculate a given resolution from the previous one instead of starting every time from the initial signal. In this algorithm:

$A_j^d f$ is computed by convolving $A_{j+1}^d f$ with H and downsampling by 2 (H = low pass filter).

$$A_j^d f(m) = \sum_{k=-\infty}^{+\infty} h(2m-k) A_{j+1}^d f(k)$$

 where $\downarrow 2$ means: retaining half of the results.

Wavelet function

To "come back" from a given resolution to the initial signal (multiresolution synthesis) it is necessary to store the lost details for each multiresolution analysis level. This is done through wavelet functions.

sum of retained parts

$$0_j \oplus V_j = V_{j+1}$$

$$\uparrow \quad \downarrow$$

 orthogonal complement of V_j and V_{j+1}
 $\hookrightarrow \psi_j$

original signal

One wavelet functions $\psi_j(x)$, $j < 0$ reconstruct the dropped information by applying $\psi_j(x)$ to $f(x)$, forming a set of bands:

$$\psi_j(x) = 2^j \psi(2^j x), j < 0$$

$$\psi_j(x) = 2^j \psi(2^j x), j > 0$$

$$\psi_j(x) = 2^j \psi(2^j x), j < 0$$

The discrete details are obtained by the projection of $f(x)$ on $\psi_j(x)$, $j < 0$:

$$D_j f(m) = \langle f(x), \psi_j(x - 2^{-j}m) \rangle_{x \in \mathbb{Z}}$$
 which can be rewritten by def. of inner product as:

$$D_j f(m) = (f(x) * \psi_j(-x))(2^{-j}m)_{m \in \mathbb{Z}}$$
 is called discrete details of $f(x)$ at resolution 2^j

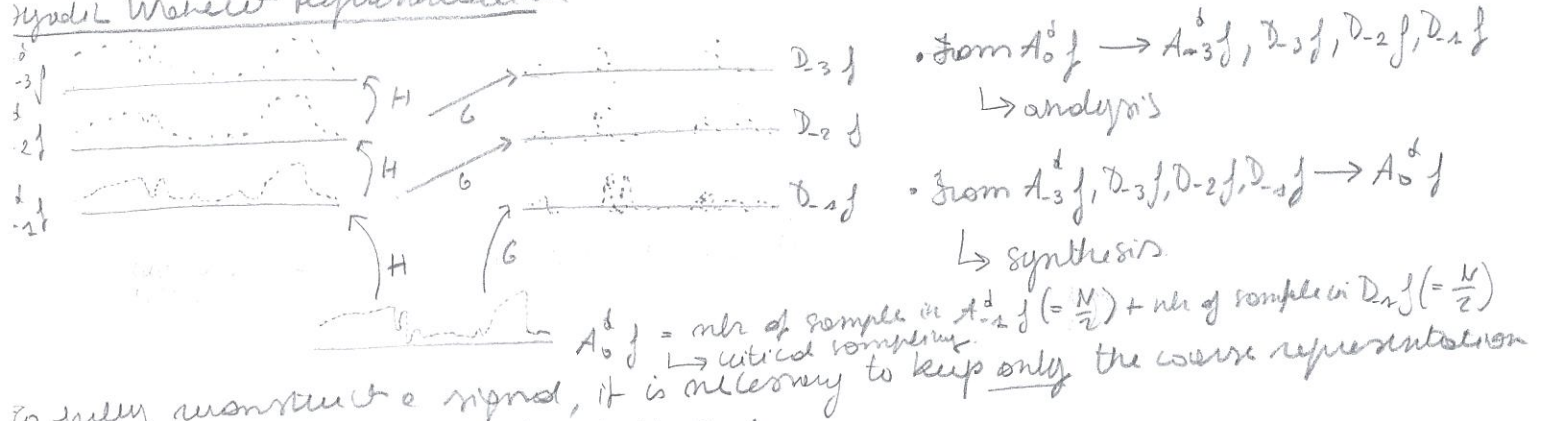
and show that it consists in a band pass filtering of $f(x)$ sampled uniformly at a rate 2^j .

the first algorithm to compute the $D_j f$ is also called the pyramid algorithm and allows to define $D_j f$ from the corresponding $A_{j+2} f$. $D_j f$ is computed by convolving $A_{j+2} f$ with G followed by a downsampling by 2 (G = band pass filter)

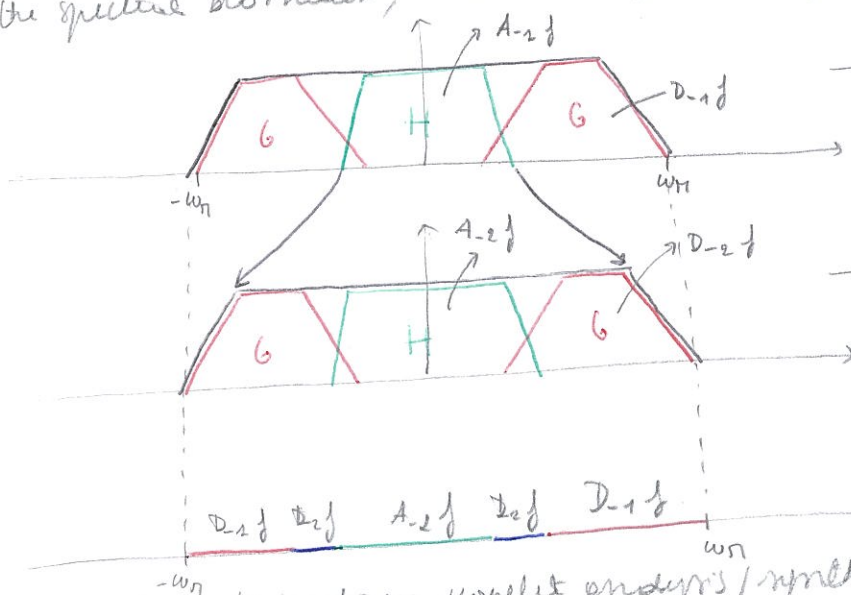
$$D_j f(m) = \sum_{k=-\infty}^{+\infty} g(2m-k) A_{j+2} f(k), j \leq 0$$

$A_0 f \rightarrow [G] \rightarrow [\downarrow 2] \rightarrow D_{-1} f$

Pyramid Wavelet Representation



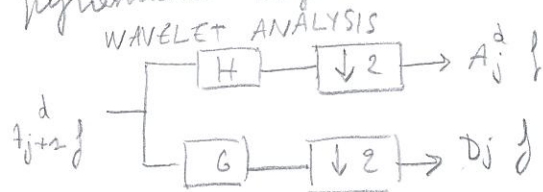
to fully reconstruct a signal, it is necessary to keep only the coarse representation of it ($A_{-3} f$) and all the lost details $D_j f$.
 In the frequency domain, this decomposition gives:



original spectrum: overlapping between H and G as non overlapping does not exist in reality (corresponds to a sinc)

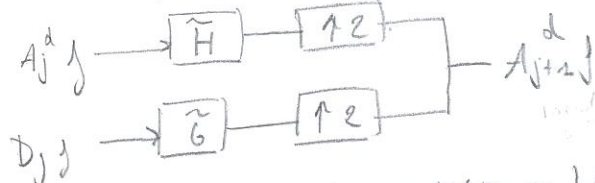
frequency band doubled as downsampling operation shrinks the time thus spread the frequency domain
 $\& R.O.O.F: F_y = \frac{F_x}{2} \rightarrow \omega_x = \frac{2\pi F}{F_x}$
 $\omega_y = \frac{2\pi F}{F_y} = 2 \cdot \frac{2\pi F}{F_x} = 2 \cdot \omega_x$

The algorithms to perform wavelet analysis/synthesis are a combination of the 2 pyramidal algorithms:



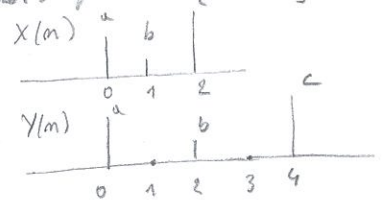
H - analysis low pass filter
 G - analysis band pass filter
 $\phi(2\omega) = H(\omega) \phi(\omega)$
 $\psi(2\omega) = G(\omega) \phi(\omega)$

WAVELET SYNTHESIS



\tilde{H} - synthesis low pass filter $= H(-h)$
 \tilde{G} - synthesis band pass filter $= G(-h)$

upsampling means



The equality $\tilde{H}(m) = H(1-m)$ holds only for orthogonal transform (critical sampling).
 This means that there are the same number of samples in the transformed domain as in the spatial domain:

Analysis: $A_0 f \xrightarrow{\text{analysis}} [A_{-1} f \oplus D_{-1} f] \xrightarrow{\text{analysis}} [A_{-2} f \oplus D_{-2} f] \xrightarrow{\text{analysis}} [A_{-3} f \oplus D_{-3} f]$

Synthesis: $[A_{-3} f \oplus D_{-3} f] \xrightarrow{\text{synthesis}} [A_{-2} f \oplus D_{-2} f] \xrightarrow{\text{synthesis}} [A_{-1} f \oplus D_{-1} f] \xrightarrow{\text{synthesis}} A_0 f$

5.4. Applications

Embedded Zerotree Coding of Wavelet Coefficients (EZW)

Organize the coefficients with similar locations in corresponding subbands in trees growing exponentially across the scales

Apply SAQ.

Zerotree hypothesis: if a coefficient is not significant with respect to a given threshold T , then all of its descendants are not significant either with respect to T .

For every T encode the resulting significance map.



90

5.4. Applications

Zerotree Representation

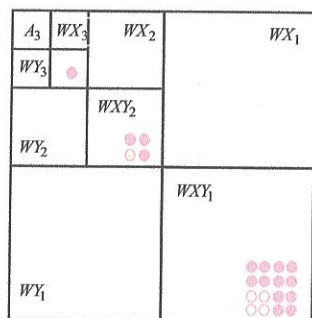
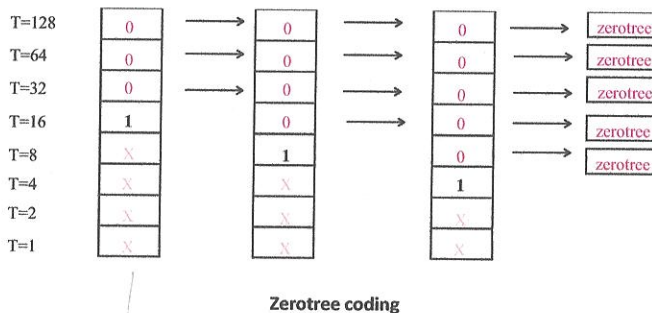


Illustration of the parent-child dependencies



Zerotree coding

for significant after column ???

- Model: the *zerotree hypothesis* is satisfied with a high probability
- The EZW coder exploits inter-band correlations.

91

5.4. Applications

Encoding Algorithm

Dominant Pass

- The subbands are scanned in Z-order.
- Raster scanning within the subbands.

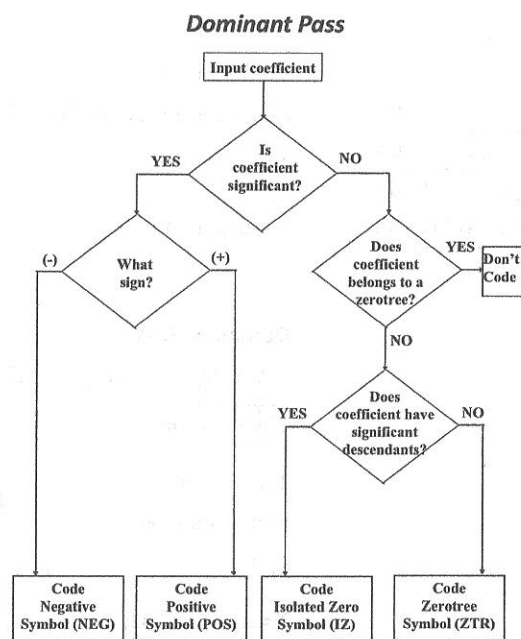
⇒ *dominant list*

Subordinate Pass.

- Applied for the coefficients that have been coded previously as significant.
- Current threshold 2^T
- For every coefficient coded as POS or NEG send to the decoder the information contained in the bit-plane T .

⇒ subordinate list

- Entropy coding of both lists.



5.4. Applications

Encoding Algorithm (example)

10	8	1	2
2	4	-1	-2
3	4	0	0
1	2	1	1

→ restart procedure with lower threshold

0	0	1	2
2	4	-1	-2
3	4	0	0
1	2	1	1

0	0	0	0
0	1	0	0
0	1	0	0
0	0	0	0

~~T=2,~~ T=1, \rightarrow next steps

Dominant Pass

POS, POS, ZTR, ZTR, ZTR, ZTR, ZTR, ZTR

10	8
----	---

Subordinate Pass

Dominant Pass

- ZTR, IZ, POS, ZTR, POS, ZTR, (ZTR), ZTR, ZTR, ZTR, ZTR

10	8	4	4
----	---	---	---

10 8

T-8

1-8

Subordinate Pass

0.0

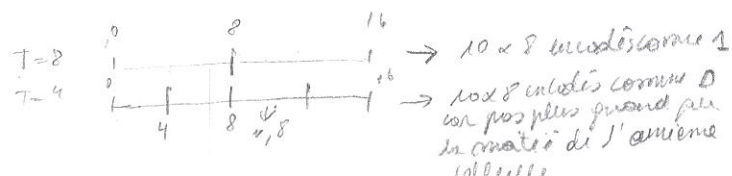
10	8
1	1
0	0
1	0
0	0

→ encoding of threshold θ

→ modeling of thresholds 4

→ Dependências

- holds the quiescent cells
- if magnitude \geq upper half of dcd cell $\rightarrow 1$
- $<$ $\rightarrow 0$



5.4. Applications

Decoding Algorithm (example)

0	0	0	0
0	0	0	0
0	0	0	0
0	0	0	0

Dominant Pass

POS, POS, ZTR, ZTR, ZTR, ZTR, ZTR, ZTR

10	8
----	---

Subordinate Pass

→ at next step, we refine, we know we have a

Dominant Pass

-, ZTR, IZ, POS | ZTR, POS, ZTR, ZTR, ZTR, ZTR, ZTR

10	8	4	4
----	---	---	---

T=8 T=4

Subordinate Pass

0, 0

T=2, T=1,

T=8

12	12	0	0
0	0	0	0
0	0	0	0
0	0	0	0

T=4

10	10	0	0
0	6	0	0
0	6	0	0
0	0	0	0

from POS and T=8, we know that the nbr to be reconstructed is between 8 and 16 (16 is the next threshold value (2^4)) and is positive. The reconstructed chosen nbr is in the middle of 8 to 16 → 12.

we know we are in the lower half of previous cell.

T=8 1 80
T=4 0

8 10 12 16

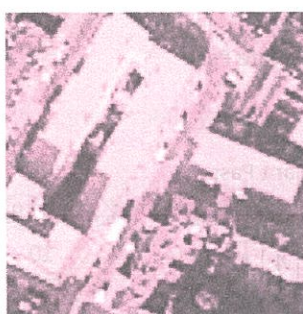
we know we have 10, bc 10 < 12 (middle of lower half of previous cell)

5.4. Applications

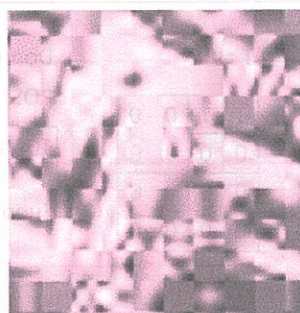
Example



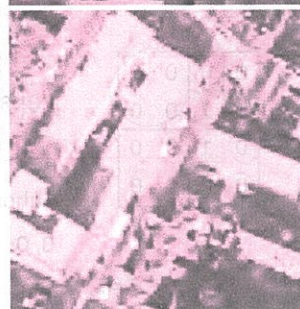
Original image



Zoomed area



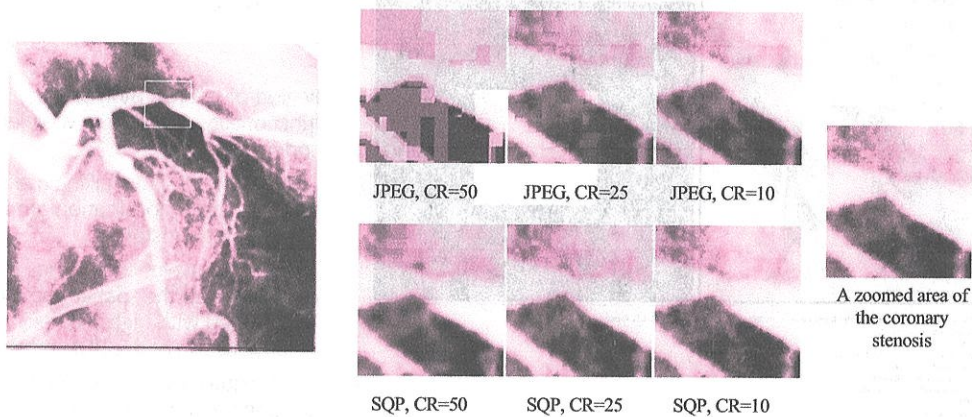
Zoomed area in the image compressed with DCT (JPEG)



Zoomed area in the image compressed with wavelets

5.4. Applications

Quality Scalability



The image on the left is compressed at 50:1, 25:1, and 10:1 with JPEG and SQP. The zoomed area of the coronary stenosis indicates by the white rectangle is progressively refined up to the lossless version depicted on the right.

Note: the wavelet codec progressively refines the decoded image as more information is received. This illustrates the quality scalability property of wavelet-based image coding.

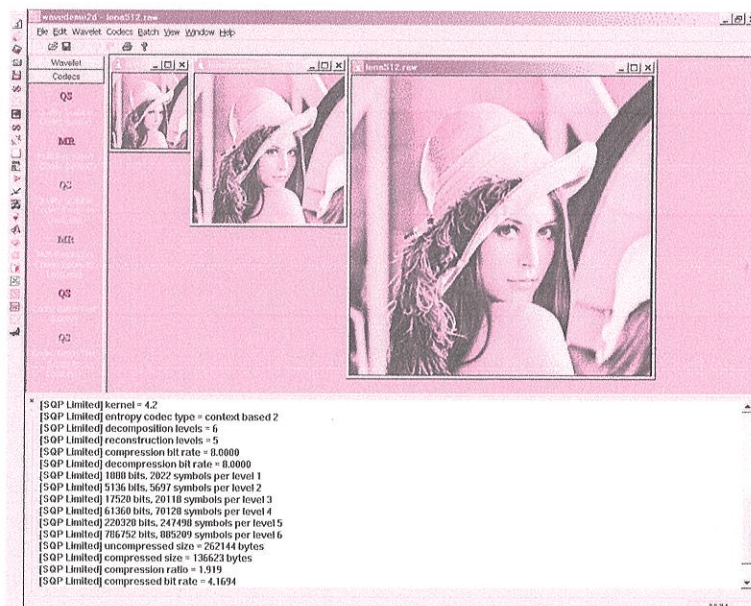
96

5.4. Applications

Resolution Scalability

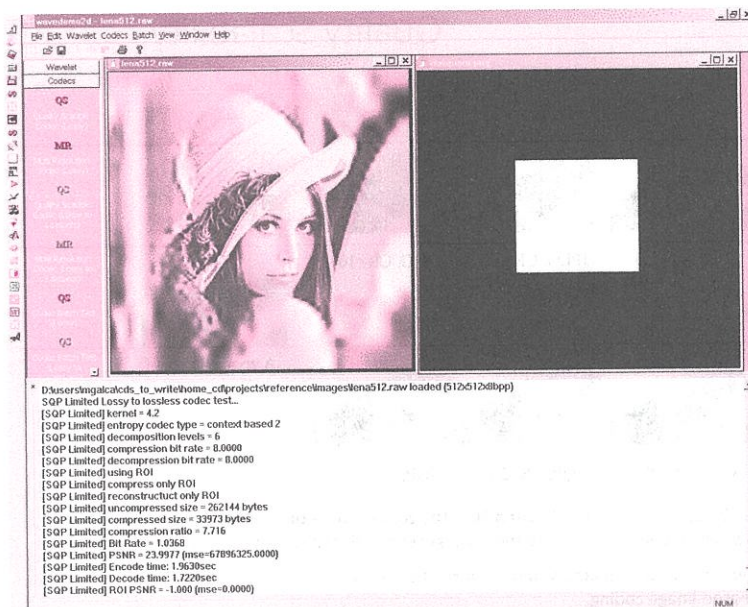
Resolution Scalability provided by wavelet-based coding

- this is obtained by progressively transmitting the wavelet subbands from the lowest to the highest resolution level



97

5.4. Applications



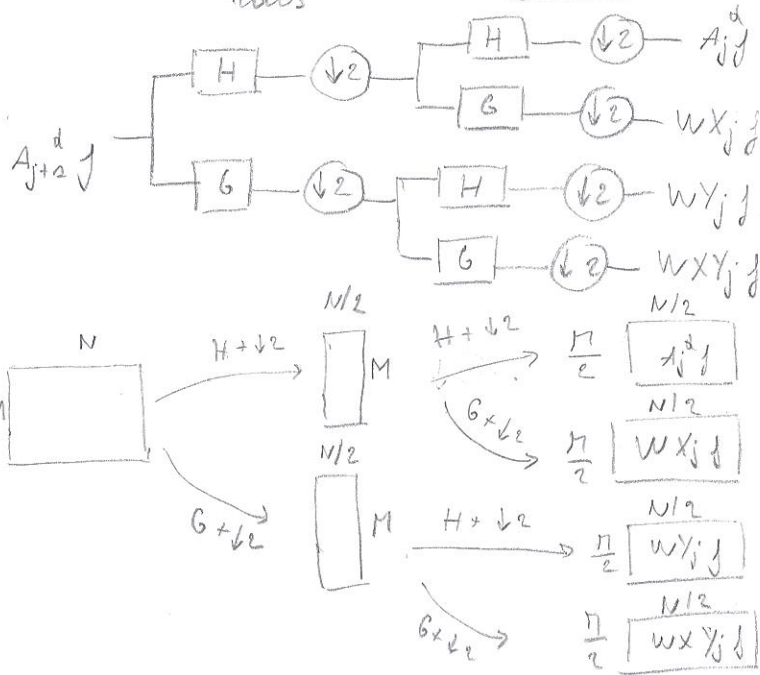
Region-of-Interest (ROI) coding

Region-of-Interest (ROI) coding functionality provided by wavelet-based coding systems

- this is obtained by making use of the time-frequency localization properties of the wavelet transform
- Only the wavelet coefficients that correspond to the spatial-domain ROI are transmitted with high accuracy (lossless reconstruction of the ROI in this example)
- A low quality version of the background is being transmitted as well
- This figure illustrates a rectangular ROI delineated by the user

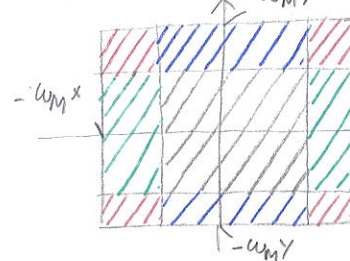
on x, y , as the mapping is considered to be reversible, it is possible to build the 2D algorithm from the combination of 1D wavelets.

2D WAVELET ANALYSIS



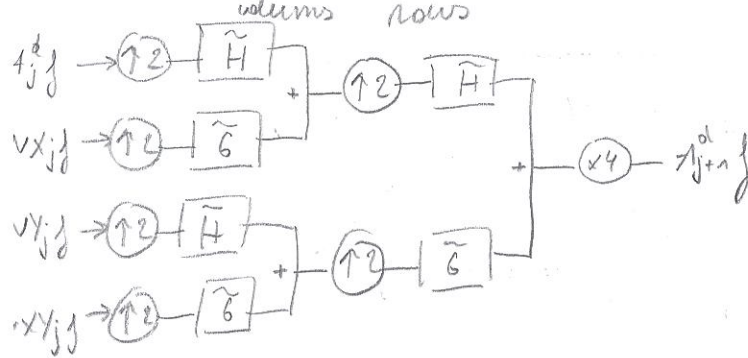
Example slide 87 (à air): the grey squares are the lost (?) details. There are 4 levels of resolutions ($4 \times$ decimés comparés à l'intervalle de 4 carrés). The most noisy square corresponds to the edges of the image. The wavelet compacts energy in some few coefficients of high amplitude.

Spatial domain:



- low pass filtering on rows & columns
- band pass filtering on columns and low pass filtering on rows
- band pass filtering on rows and low pass filtering on columns
- band pass filtering on rows & columns

2D WAVELET SYNTHESIS



Applications

Embedded Zerotree Coding of Wavelet Coefficients (EZWC)
 This technique deals with the efficient coding of the significance maps. These maps are sets of binary maps indicating the position of significant coefficients. They indicate the values above a threshold fixed by the embedded quantizer and their location. To do that in a fast way, zerotree hypothesis is used. It states that if there are zeros in a certain zone of the image details at a given resolution, there is a high likelihood that the corresponding coefficient in the next resolution level will be zeros too, forming a zerotree. This hypothesis comes from the $1/f$ tendency, stating that there is a higher chance to have important coefficient at low freq than at high frequency.

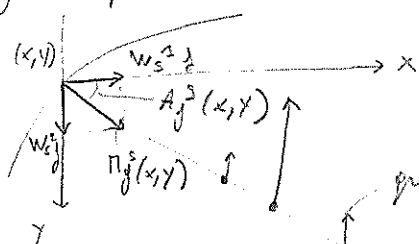
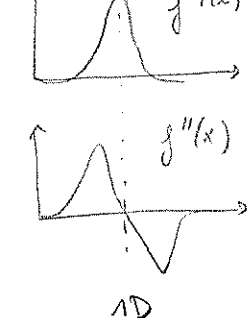
The input picture is first analyzed through wavelet then quantized with SAT.

→ improve slide 80 from analysis.

- Quality stability
cf slides 86
- Resolution stability
cf slide 87
- Region-of-interest stability
cf slide 88

• Multi-scale edge detection via CWT

An edge is defined as an inflexion point on the function describing the image (image?)
 To find the inflexion point, the wavelet uses $f'(x)$ as it has a maximum at this point. In 2D, edges are thus defined as a local maximum of the gradient (2D $f'(x)$) magnitude in the gradient direction.



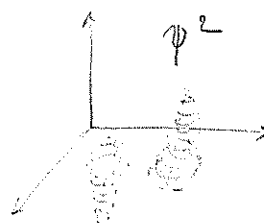
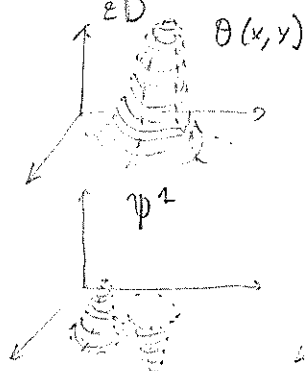
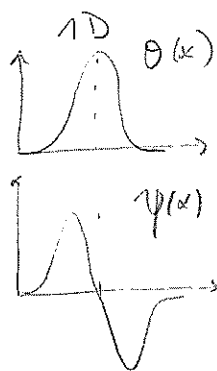
In every point (x, y) , there are 2 wavelet information: the magnitude and the angle
 $\nabla f^s(x, y)$ (magnitude)
 $A_f^s(x, y)$ (angle)

gradient magnitude
 gradient direction

In order to perfectly detect the edge, it is important to first suppress the noise of the image because otherwise, edges are found everywhere.
 To detect it, the image is convolved with a smoothing filter: $\Theta_s(x) = \frac{1}{s} \Theta(\frac{x}{s})$
 The corresponding wavelet for edge detection is $\psi(x) = \frac{d}{dx} (\Theta(x))$, $\psi_s(x) = \frac{1}{s} \psi(\frac{x}{s})$

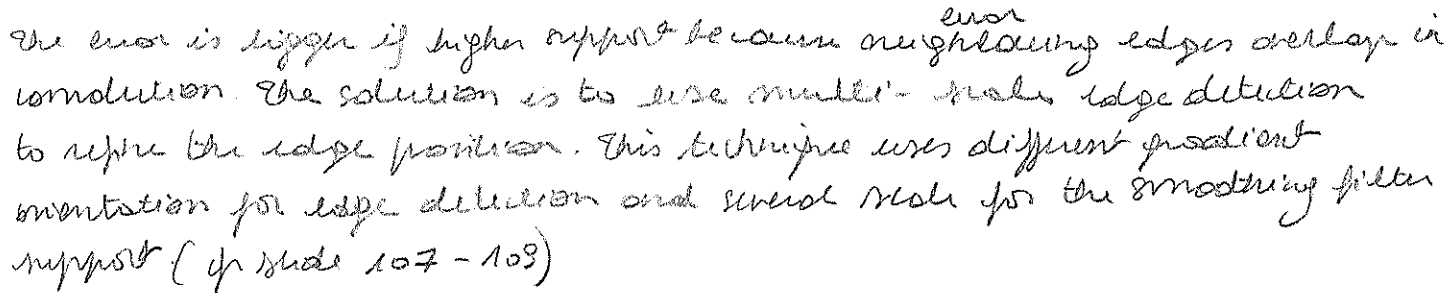
In 2D, the smoothing function is: $\Theta(x, y) = \Theta(x) \cdot \Theta(y)$
 the wavelet functions are: $\psi^2(x, y) = \frac{d}{dx} \Theta(x, y)$, $\psi^2(x, y) = \frac{d}{dy} \Theta(x, y)$
 the 2D wavelet transforms are: $W_s^2 f(x, y) = (f * \psi_s^2)(x, y) = s \frac{d}{dx} (f * \Theta_s)(x, y)$
 $W_s^2 f(x, y) = (f * \psi_s^2)(x, y) = s \frac{d}{dy} (f * \Theta_s)(x, y)$

The modulus and angle of $\nabla(f * \Theta_s)$ at (x, y) is: $\nabla f^s(x, y) = (W_s^2 f(x, y))^2 + (W_s^2 f(x, y))^2$
 $A_f^s(x, y) = \arg(W_s^2 f(x, y) + j W_s^2 f(x, y))$



The problem is that this changes the position of the edges. bigger the support of the smoothing filter, better the detection of the noise but worst is the error on edge location. Indeed if the signal is and the filter is → response to remove noise → find location → error location

a the film is



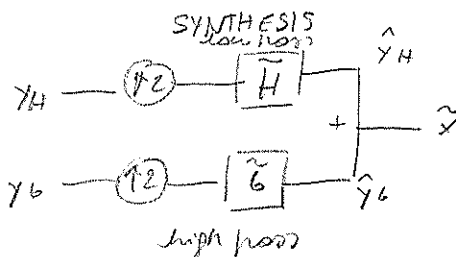
WAVELET BASES & FILTER BANKS
 Perfect reconstruction filter banks implement series expansions of discrete-time signals.
 There are 3 types of tools for analysing filter banks: time domain analysis,
 modulation domain analysis, polyphase domain analysis.

Two channel Filter Banks - Modulation domain

If the system is continuous \rightarrow Laplace transform to solve CWT

If the system is discrete \rightarrow Z transform to solve CWT

SYNTHESIS



The distinct domain will be represented in this case:

• convolution of discrete signals: $\mathcal{Z} \{ x[m] * y[m] \} = X(z) \cdot Y(z)$

PROOF: $X(z) \cdot Y(z) = \left(\sum_{n=-\infty}^{\infty} x[n] z^{-n} \right) \left(\sum_{m=-\infty}^{\infty} y[m] z^{-m} \right) = \sum_{h=-\infty}^{\infty} \sum_{l=-\infty}^{\infty} x[l] y[l-h] z^{-h}$

Unter der Bedingung $n + m = 10$

$$= \sum_{p=0}^{\infty} \sum_{m=0}^{\infty} x [p-m] y [m] z^{-p} = \sum_{p=0}^{\infty} \left(\sum_{m=0}^{\infty} x [p-m] y [m] \right) z^{-p} \quad (4)$$

$$W(p) = \sum_{m=0}^{\infty} u(p-m) y(m) \triangleq u(p) \otimes y(p)$$

from (4), we deduce $X(z) \cdot Y(z) = S(z)$

since $\pm(x[m] * y[m]) = X(z) \cdot Y(z)$

• downsampling of discrete signals: $y[n] = x[2n] \rightarrow \mathcal{Z}(y[n]) = Y(z) = \frac{1}{2} [X(z^{1/2}) + X(-z^{1/2})]$

PROOF: let $X_e(z) = \sum_{n=0}^{\infty} x[n] z^{-n}$ and $X_o(z) = \sum_{n=0}^{\infty} x[n+1] z^{-n}$

thus $Y(z) = \sum_{n=0}^{\infty} y[n] z^{-n} = \sum_{n=0}^{\infty} x[n] z^{-n} = X(z)$

$$\text{also } X(z) = \sum_{k=0}^{\infty} u[k] z^{-k} = \sum_{k=0}^{\infty} u[2m] z^{-2m} + \sum_{m=0}^{\infty} u[2m+1] z^{-(2m+1)}$$

$$= X_p(z^2) + z^{-1} X_o(z^2) \quad (4)$$

upholing $z \rightarrow -z$

$$X(-z) = X_e(z^2) - z^{-1} X_o(z^2) \quad (7.7)$$

from (*) and (**) it results: $X_e(z) = \frac{1}{2} [X(z) + X(-z)] \Rightarrow X_e(z) = 1/2 [X(z^{1/2}) + X(-z^{1/2})]$

$$X_o(z) = \frac{z}{2} [X(z) - X(-z)] \Rightarrow X_o(z) = \frac{z^{1/2}}{2} [X(z^{1/2}) - X(-z^{1/2})]$$

$X_e(z), X_o(z)$ represents the Z transforms of the even and odd phases of the input signal $x[n]$

upsampling discrete signals: $y[2m] = x[m], y[2m+1] = 0$ thus $\tilde{X}(y) = Y(z) = X(z^2)$

PROOF: $Y(z) = \sum_{n=-\infty}^{\infty} y[n] z^{-n} = \sum_{m=-\infty}^{\infty} y[2m] z^{-2m} + \sum_{m=-\infty}^{\infty} y[2m+1] z^{-(2m+1)} = \sum_{m=-\infty}^{\infty} x[m] z^{-2m} + 0 = X(z^2)$

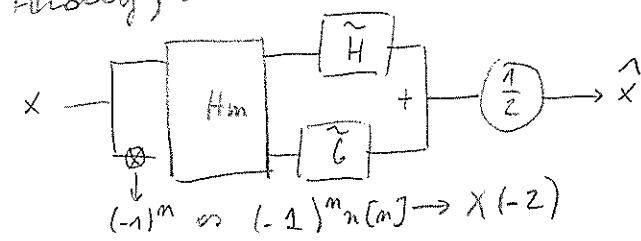
from these results we obtain that:

ANALYSIS: $Y_H(z) = \frac{1}{2} [H(z^{1/2}) X(z^{1/2}) + H(-z^{1/2}) X(-z^{1/2})]$
 $Y_L(z) = \frac{1}{2} [G(z^{1/2}) X(z^{1/2}) + G(-z^{1/2}) X(-z^{1/2})]$
 $\Rightarrow Y(z) = \frac{1}{2} H_m(z^{1/2}) X_m(z^{1/2})$

SYNTHESIS: $\hat{Y}_H(z) = \tilde{H}(z), Y_H(z^2) = \frac{1}{2} \tilde{H}(z) [H(z) X(z) + H(-z) X(-z)]$
 $\hat{Y}_L(z) = \tilde{G}(z), Y_L(z^2) = \frac{1}{2} \tilde{G}(z) [G(z) X(z) + G(-z) X(-z)]$
 $\hat{X}(z) = \hat{Y}_H(z) + \hat{Y}_L(z) = \frac{1}{2} \underbrace{\begin{pmatrix} \tilde{H}(z) & \tilde{G}(z) \end{pmatrix}}_{H_m(z)} \underbrace{\begin{pmatrix} H(z) & H(-z) \\ G(z) & G(-z) \end{pmatrix}}_{X_m(z)} \begin{pmatrix} X(z) \\ X(-z) \end{pmatrix} \quad (I)$

H_m is the analysis modulation matrix.

Finally, the modulation-domain analysis of the two-channel filter bank gives



$(-1)^m \Rightarrow (-1)^m x[n] \rightarrow X(-z)$

\rightarrow upsample analysis, then decimate by 2 and average.

the perfect reconstruction condition is expressed as:

$\hat{X}(z) = X(z) \Rightarrow \begin{cases} \tilde{H}(z) H(z) + \tilde{G}(z) G(z) = 2 & \text{from (I)} \\ \tilde{H}(z) H(-z) + \tilde{G}(z) G(-z) = 0 & \text{matrix isolation} \end{cases} \rightarrow \begin{pmatrix} \tilde{H}(z) & \tilde{G}(z) \end{pmatrix} H_m(z) = \begin{pmatrix} 2 & 0 \end{pmatrix}$

By transposing this relation and multiplying by $(H_m^T(z))^{-1}$ we obtain:

$\begin{pmatrix} \tilde{H}(z) \\ \tilde{G}(z) \end{pmatrix} = \frac{2}{\det(H_m(z))} \begin{pmatrix} G(-z) \\ -H(-z) \end{pmatrix}$ (det isn't 0 as $H_m(z)$ is invertible)

Defining $P(z) = \tilde{H}(z) H(z) = \frac{2}{\det(H_m(z))} H(z) G(-z) \rightarrow$ in current $\tilde{H}(z)$ & $\tilde{G}(z)$ are the analysis filters

$\tilde{G}(z) G(z) = \frac{-2}{\det(H_m(z))} H(-z) G(z) = P(-z)$ because $\det(H_m(z)) = -\det(H_m(-z))$

the perfect reconstruction condition is expressed as

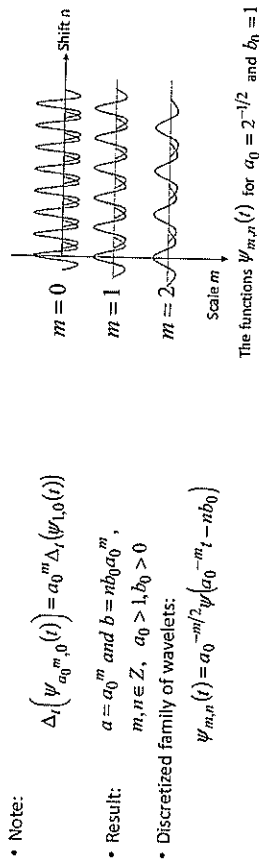
$P(z) + P(-z) = 2$
 \rightarrow polynomial with coefficients of discrete-time signals can be implemented easily

HW: proof that $H(z) = \sum_{n=-\infty}^{\infty} h[n] z^{-n} \rightarrow H(z) = \frac{\sqrt{2}}{2} (1+z^{-1})$ with $h[n] = \frac{\sqrt{2}}{2}$

$\hookrightarrow \sum_{n=0}^{\infty} z^{-n} =$

4.3.1. Discretization of CWT

- Discretization of the scale parameter
 $a = a_0^m, m \in \mathbb{Z}, a_0 \neq 1$
- Discretization of the time shift
First idea: For $m = 0$, take $b = nb_0$
 Choose b_0 such that $\psi_{1,b} = \psi(t - nb_0)$ covers the whole time axis
 Moreover, choose b_0 such that for any m , $\psi_{a_0^m, b}(t)$ covers the whole time axis.



50

4.3.2. Discretization of STFT

Discretization of the frequency parameter

$$\omega = m\omega_0, \omega_0 > 0, m \in \mathbb{Z}, \omega_0 \text{ fixed}$$

Discretization of the time shift

$$\tau = n\tau_0, \tau_0 > 0, n \in \mathbb{Z}, \tau_0 \text{ fixed}$$

Result:

$$g_{\omega,\tau}(t) \rightarrow g_{m,n}(t) = e^{jm\omega_0 t} g_1(t - n\tau_0)$$

Note:

$$\Delta_t(g_{m,0}(t)) = \Delta_t(g_1,0(t))$$

$$\Delta_\omega(g_{m,0}(t)) = \Delta_\omega(g_1,0(t))$$

Different sampling grid for the discretization of the STFT if compared with the CWT

Let's come back to the problem:

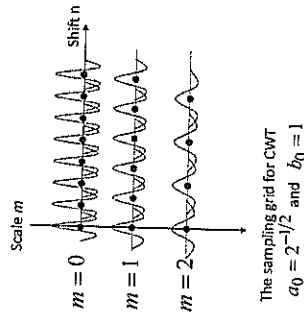
$$\text{Given } \{g_{m,n}, f\}, \text{ in which conditions } f = \sum_m \sum_n \langle g_{m,n}, f \rangle \tilde{g}_{m,n}$$

$$\text{Given } \{\psi_{m,n}, f\}, \text{ in which conditions } f = \sum_m \sum_n \langle \psi_{m,n}, f \rangle \tilde{\psi}_{m,n}$$

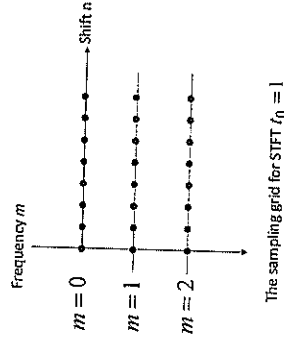
51

4.3.1. Discretization of CWT

Sampling grid for the CWT



Sampling grid for the STFT



51

4.3.3. Reconstruction in Frames

What is necessary to have a stable reconstruction?

$$1. \quad f(t) \xrightarrow{\text{operator}} \langle \psi_{m,n}(t), f(t) \rangle$$

This operator should be bounded: $f(t) \in L^2(\mathbb{R}) \Rightarrow \sum_{m,n} |\langle \psi_{m,n}, f \rangle|^2$ is finite

It can be shown that $\exists B \in \mathbb{R}^+$, such that $\sum_{m,n} |\langle \psi_{m,n}, f \rangle|^2 \leq B \|f\|^2$

2. Intuitively, if $\|f\|^2$ is small $\Rightarrow \sum_{m,n} |\langle \psi_{m,n}, f \rangle|^2$ is small too \Rightarrow

\Rightarrow If $\sum_{m,n} |\langle \psi_{m,n}, f \rangle|^2 < 1 \Rightarrow \exists \alpha \in \mathbb{R}$, such that $\|f\|^2 \leq \alpha$

Define $\tilde{f} = \frac{f}{\sqrt{\sum_{m,n} |\langle \psi_{m,n}, f \rangle|^2}}$ for an arbitrary f in $L^2(\mathbb{R})$

It can be shown that $\sum_{m,n} |\langle \psi_{m,n}, \tilde{f} \rangle|^2 \leq 1 \Rightarrow \exists \alpha' \in \mathbb{R}$, such that $\|\tilde{f}\|^2 \leq \alpha'$

This implies: $\frac{1}{\alpha'} \|f\|^2 \leq \sum_{m,n} |\langle \psi_{m,n}, f \rangle|^2 \Leftrightarrow A \|f\|^2 \leq \sum_{m,n} |\langle \psi_{m,n}, f \rangle|^2$

53

4.3.3. Reconstruction in Frames

- Reconstruction is possible if the family $(\psi_{m,n})_{m,n \in \mathbb{Z}}$ constitutes a frame.

$$\exists A, B, 0 < A \leq B < \infty, \quad A \cdot \|f\|^2 \leq \sum_{m,n} |\langle \psi_{m,n}, f \rangle|^2 \leq B \cdot \|f\|^2$$

- Note: take $f = f_1 - f_2$. First inequality means that the distance $\|f_1 - f_2\|$ cannot be arbitrarily large if is small: stability requirement.
- When $A = B$, the frame is tight.

Proposition

If $A = B = 1$ and $\forall m, n \in \mathbb{Z}, \|\psi_{m,n}\| = 1$, the family $(\psi_{m,n})_{m,n \in \mathbb{Z}}$ is an orthonormal basis.

- $A = B$ gives the "redundancy ratio", or the oversampling ratio.
- $A = B = 1 \Rightarrow$ critical sampling \Leftrightarrow orthonormal basis.

54

4.3.3. Reconstruction in Frames

A. Reconstruction in tight frames

$$\begin{aligned} \sum_{m,n} |\langle \psi_{m,n}, f \rangle|^2 &= A \|f\|^2 \Leftrightarrow \sum_{m,n} \langle f, \psi_{m,n} \rangle \cdot \langle \psi_{m,n}, f \rangle = A \langle f, f \rangle \\ \sum_{m,n} \langle f, \psi_{m,n} \rangle \cdot \langle \psi_{m,n}, f \rangle &= \sum_{m,n} \langle f, \psi_{m,n} \rangle \cdot \int \psi_{m,n}^*(t) f(t) dt = \\ &= \int \left(\sum_{m,n} \langle f, \psi_{m,n} \rangle \cdot \psi_{m,n}^*(t) \right) \cdot f(t) dt = \left(\sum_{m,n} \langle f, \psi_{m,n} \rangle \cdot \psi_{m,n}^* \right) \cdot f = A \langle f, f \rangle \\ &\Rightarrow f = \frac{1}{A} \sum_{m,n} \langle f, \psi_{m,n} \rangle \cdot \psi_{m,n} = \frac{1}{A} \sum_{m,n} \langle \psi_{m,n}, f \rangle \cdot \psi_{m,n} \end{aligned}$$

A frame, even a tight frame is not an orthonormal basis. It is a set of non-independent vectors.

Example:

- Consider \mathbb{R}^2 and a redundant set of vectors:

$$\varphi_0 = [1, 0]^T, \varphi_1 = [-1/2, \sqrt{3}/2]^T, \varphi_2 = [-1/2, -\sqrt{3}/2]^T$$

55

4.3.3. Reconstruction in Frames

Example:

- Create $M = [\varphi_0, \varphi_1, \varphi_2]$. One can verify that: $MM^T = \frac{3}{2} I \Rightarrow \forall x \in \mathbb{R}^2, x = \frac{2}{3} \sum_{i=0}^2 \langle \varphi_i, x \rangle \varphi_i$

- Note that $\|\varphi_i\|_{i=0,1,2} = 1$ and $3/2$ is the redundancy factor. The vectors are linearly dependent:

B. Reconstruction in frames that are not tight

Proposition $\exists a, b$, such that: $\varphi_0 = a \cdot \varphi_1 + b \cdot \varphi_2 \Rightarrow a = b = -1$

Given a family of functions $(\gamma_j)_{j \in J}$ that constitutes a non-tight frame in a Hilbert space H , there exists a family of functions $(\tilde{\gamma}_j)_{j \in J}$ called a dual frame, satisfying:

$$B^{-1} \|f\|^2 \leq \sum_{j \in J} |\langle \tilde{\gamma}_j, f \rangle|^2 \leq A^{-1} \|f\|^2, \text{ and}$$

$$f = \sum_{j \in J} \langle \gamma_j, f \rangle \tilde{\gamma}_j = \sum_{j \in J} \langle \tilde{\gamma}_j, f \rangle \gamma_j$$

56

4.3.4. Frames of the CWT

Proposition

If $\psi_{m,n}(t) = a_0^{-m/2} \psi(a_0^{-m} t - nb_0)$, $m, n \in \mathbb{Z}$ constitutes a frame in $L^2(\mathbb{R})$ with frame bounds A, B , then:

$$\text{Admissibility condition: } \frac{b_0 \ln a_0}{2\pi} A \leq \int_0^\infty \frac{|\Psi(\omega)|^2}{\omega} d\omega \leq \frac{b_0 \ln a_0}{2\pi} B \quad \text{and} \quad \frac{b_0 \ln a_0}{2\pi} A \leq \int_{-\infty}^0 \frac{|\Psi(\omega)|^2}{|\omega|} d\omega \leq \frac{b_0 \ln a_0}{2\pi} B$$

The wavelets form a frame \Rightarrow admissibility condition is automatically satisfied.

$$\text{Frame bounds for tight frames: } C_\psi = \int_{-\infty}^\infty \frac{|\Psi(\omega)|^2}{|\omega|} d\omega < \infty$$

For orthonormal bases (e.g. the dyadic case), the wavelet should satisfy:

$$A = B = \frac{2\pi}{b_0 \ln a_0} \int_0^\infty \frac{|\Psi(\omega)|^2}{\omega} d\omega = \frac{2\pi}{b_0 \ln a_0} \int_{-\infty}^0 \frac{|\Psi(\omega)|^2}{|\omega|} d\omega$$

$$A = B = 1, a_0 = 2, b_0 = 1, \quad \int_0^\infty \frac{|\Psi(\omega)|^2}{\omega} d\omega = \int_{-\infty}^0 \frac{|\Psi(\omega)|^2}{|\omega|} d\omega = \frac{\ln 2}{2\pi}$$

57

4.3.3

4.3.4. Frames of the CWT

Example - Mexican Hat wavelet frames

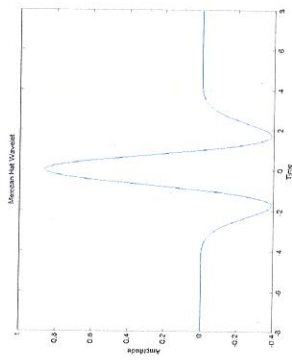
$$\psi(t) = \frac{2}{\sqrt{3}} \pi^{-1/4} (1-t^2)e^{-t^2/2}$$

b_0	A	B	B/A
0.25	13.091	14.183	1.083
0.50	6.546	7.092	1.083
0.75	4.364	4.728	1.083
1.00	3.223	3.596	1.116
1.25	2.001	3.454	1.726
1.50	0.325	4.221	12.986

For some values of b_0 the frame is almost tight.

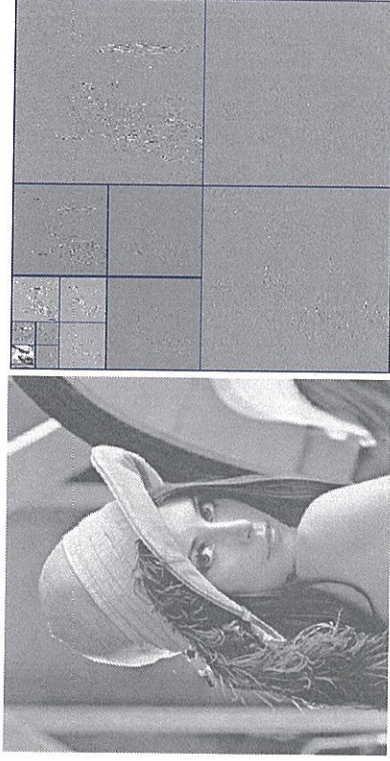
When the frame is almost tight, the frame bounds are inversely proportional to b_0 : when b_0 is halved (twice as many points on the grid), the frame bounds should double - redundancy increases by two.

For b_0 higher than 1.50 the set $\{\psi_{m,n}\}_{m,n \in \mathbb{Z}}$ is not a frame anymore: $A < 0$



5.3. The 2D Wavelet Representation

Example 2-D Wavelet Analysis

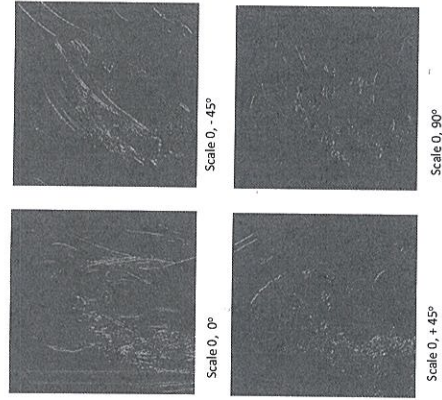


5.4 Applications

Intermediary Results

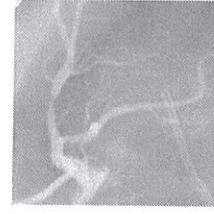


Different scales,
Different gradient
orientations

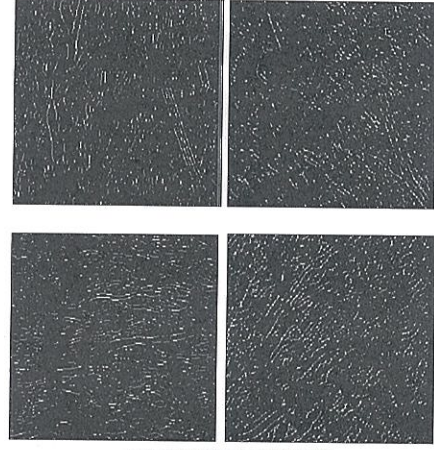


5.4 Applications

Intermediary Results



Coronary Angiogram



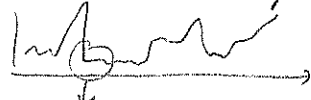
(most applications (analysis, compression, noise-removal) exploit the ability of wavelet bases to efficiently approximate particular classes of functions with few non-zero coefficients. A function f has few non-zero coefficients if most of the fine-scale wavelet coefficients are small (close to zero). Hence, the design of ψ must be optimized to produce a minimum number of coefficients $\langle f, \psi \rangle$ that are close to zero. This depends mostly on the regularity of f , the number of vanishing moments of ψ and the size of its support. order of vanishing moments

The number of vanishing moments is defined as $\int_{-\infty}^{\infty} \psi(x) x^p dx = 0 \quad p \in \mathbb{P}$

If this order is low \rightarrow lots of polynomials order of the signal kept \rightarrow loose approximation
 high \rightarrow polynomials of high order of the signal kept \rightarrow lot of information
large file

The polynomial is the function defined to fit the best the signal:

$$f(x) = a_0 + a_1 x + a_2 x^2 + \dots + a_k x^k + \dots$$



discontinuities cannot be modelled.

It is thus important to have a high order of vanishing moment but then we lose locality.

CHAPTER 4: IMAGE ENHANCEMENT

Image Enhancement is the art of playing with a broad set of available image processing tools, tuning their parameters and combining them in a skillful way. The goal is to improve the appearance of images to human viewers and to enhance the performance of subsequent image processing tools. Different methods exist such as contrast and/or dynamic range modification (dynamic range is the range spanned by the pixel gray values), noise reduction and/or edge enhancement or pseudo-coloring.

HISTOGRAM

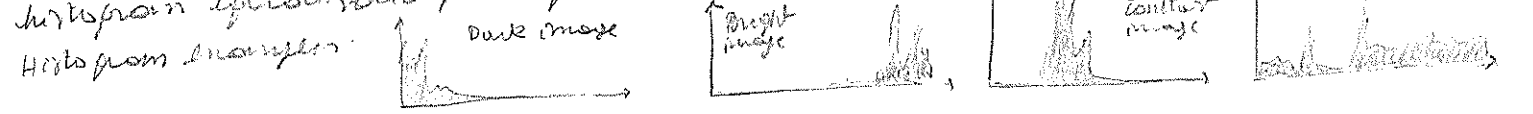
The histogram reflects the occupation level of the gray values in the image. The cumulative histogram reflects the percentage of pixels with a gray value $i \leq g$.

Here: $i \leq g \rightarrow H(g) = \sum_{i=0}^g h(i)$

Example slide 3 is wit!

CONTRAST AND DYNAMIC RANGE MODIFICATION

The quality of an image can be enhanced by modifying its histogram, i.e. applying a specific transformation in order to give to the histogram a desired shape. The following histogram control methods will be explained: histogram stretching, histogram equalization, selective histogram equalization.



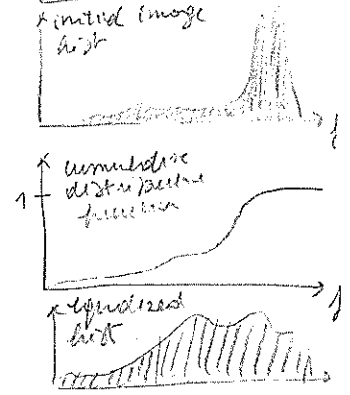
Histogram stretching

The idea is the process by which the overall dynamic range of the image intensities is increased. The result is a stretched histogram.

Histogram equalization

The processed histogram is aimed to be constant. It can be proven that this result can be obtained by using the cumulative distribution function of the input image as the transformation function.

Example 1



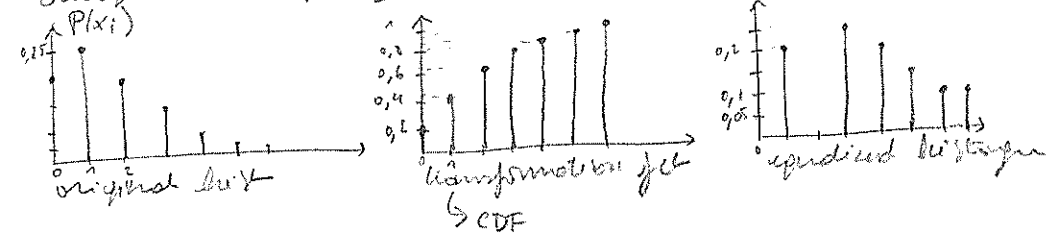
Example 2

Probabilities

$P(0) = 0,2$
$P(1) = 0,25$
$P(2) = 0,2$
$P(3) = 0,15$
$P(4) = 0,1$
$P(5) = 0,06$
$P(6) = 0,03$
$P(7) = 0,01$

CDF	Actual CDF values	Mapped values
$CDF(0) = 0,2$	$0,125 \rightarrow (0)$	$1, P'(1) = 0,2 = P(0)$
$CDF(1) = 0,45$	$0,25 \rightarrow (1)$	$3, P'(3) = 0,25 = P(1)$
$CDF(2) = 0,65$	$0,375 \rightarrow (2)$	$4, P'(4) = 0,2 = P(2)$
$CDF(3) = 0,8$	$0,5 \rightarrow (3)$	$5, P'(5) = 0,15 = P(3)$
$CDF(4) = 0,9$	$0,625 \rightarrow (4)$	$6, P'(6) = 0,1 = P(4)$
$CDF(5) = 0,96$	$0,75 \rightarrow (5)$	$7, P'(7) = 0,06 = P(5)$
$CDF(6) = 0,99$	$0,875 \rightarrow (6)$	$7, P'(7) = 0,03 = P(6)$
$CDF(7) = 1$	$1 \rightarrow (7)$	$7, P'(7) = 0,01 = P(7)$

Through this mapping, we have:



choice of scaling $P'(7)$

$$= P(5) + P(6) + P(7)$$

$$= 0,06 + 0,03 + 0,01$$

$$= 0,1$$

Histogram of an image

$n_c = 7$

1	3	2	4	3	2	1
2	2	3	4	1	3	2
3	4	4	4	1	1	2
3	2	1	4	1	3	2
2	2	2	3	3	4	1

$n_R = 5$

Pixel value: g	No pixels: $N(g)$	$N(g)/N$
1	8	23%
2	11	31%
3	9	26%
4	7	20%
	35	

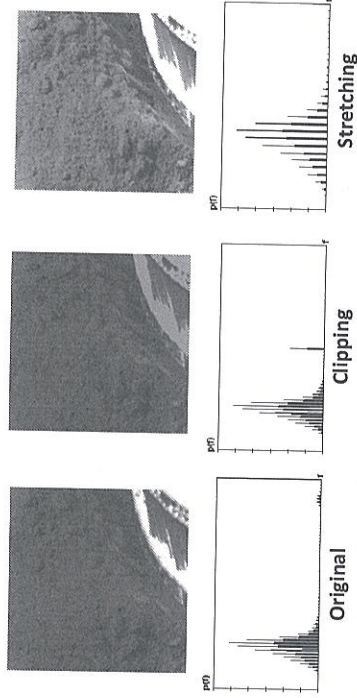
The histogram shows the percentage of pixels having a certain grey value: $h(g) = N(g)/N$

Is an estimate for the probability for grey value g

Alternative Histogram Modification techniques (1/2)

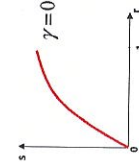
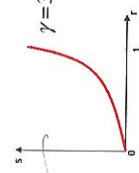
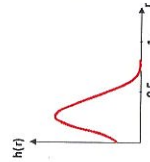
Recipe for clipping before stretching:

1. Clip the pixel gray values to a range [0,128]
2. Stretch the clipped image



Alternative Histogram Modification techniques: γ -correction (2/2)

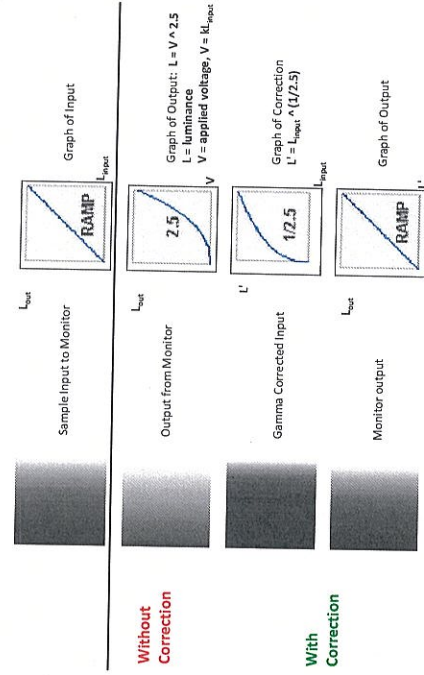
Mapping function:
with r being normalised between 0 and 1



enhanced
toward dark
pixels

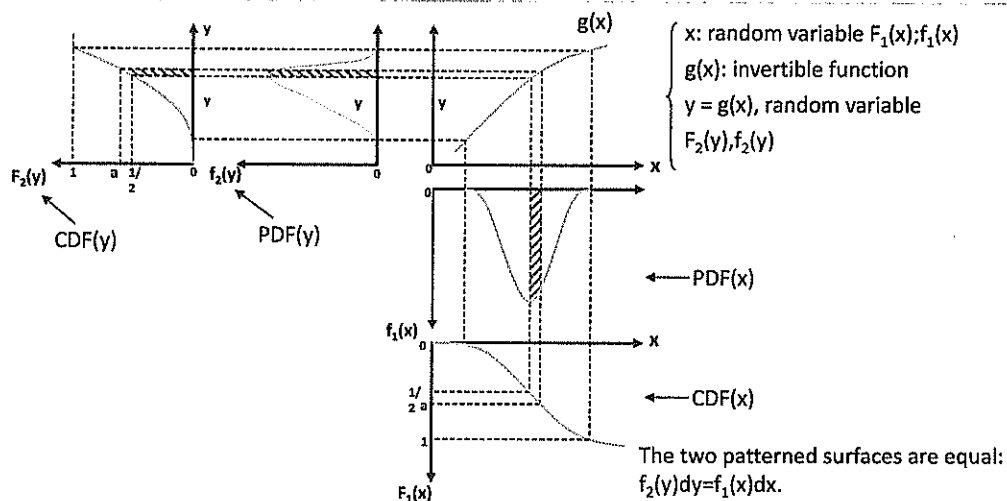
$\gamma = 0.33 \rightarrow$ enhanced
toward light pixels

Gamma Correction for CRT-Monitors



EXAMPLE

The CDF is the transform to be used in histogram equalisation



$\forall y$ for which g^{-1} exists:

$$F_2(y) = P(y \leq y) = P[x \leq g^{-1}(y)] = F_1[g^{-1}(y)] \quad (*)$$

For the probability distribution functions, we derive:

$$f_1(x) = \frac{dF_1(x)}{dx} \quad \text{and} \quad f_2(y) = \frac{dF_2(y)}{dy},$$

$$f_2(y) = \frac{dF_2(y)}{dy} = \frac{dF_1[g^{-1}(y)]}{dg^{-1}(y)} \frac{dg^{-1}(y)}{dy} = f_1[g^{-1}(y)] \frac{dg^{-1}(y)}{dy} = f_1(x) \frac{dx}{dy}$$

If we wish $f_2(y)$ to be uniform, what should we use for $g(\cdot)$?

$$\begin{cases} 0 \leq y \leq 1 \rightarrow f_2(y) = 1 \\ \text{otherwise} \quad f_2(y) = 0 \end{cases} \Rightarrow dy = f_1(x) dx \Leftrightarrow y = \int_0^x f_1(t) dt$$

$$\Leftrightarrow y = g(x) = F_1(x) = cdf(x)$$

Notice also that: $F_2(y) = F_1[g^{-1}(y)] = F_1[F_1^{-1}(y)] = y$

Conclusion: $y = g(x) = F_1(x)$ maps $f_1(x)$ towards a uniform distribution $f_2(y)$

$x = g^{-1}(y) = F_1^{-1}(y)$ maps a uniform distribution $f_2(y)$ towards $f_1(x)$

Slide 15 à être revue par le professeur mais à aller voir

Adaptive histogram equalization

the problem of histogram equalization is that it is often difficult to distinguish between low contrast details and noise. The problem of adaptive histogram equalization is:

- calculate an histogram and spreadize over a window around the pixel of interest
- wrap an a priori defined characteristic value (e.g. median) of the equalized histogram to the pixel of interest.

Other techniques also exists such as clipping + stretching (see slide 18) or γ -correction (see slide 19-20)

NOISE REDUCTION = EDGE ENHANCEMENT

Linear filtering

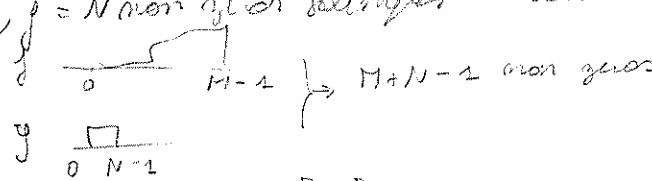
• continuous: convolution of f with a filter g : $f(x,y) * g(x,y) = \int_{-\infty}^{+\infty} \int_{-\infty}^{+\infty} f(\alpha,\beta) g(x-\alpha, y-\beta) d\alpha d\beta$

$= \int_{-\infty}^{+\infty} \int_{-\infty}^{+\infty} f(x-s, y-t) g(s,t) (-ds) (-dt)$ with $\begin{cases} s = x-\alpha \\ t = y-\beta \end{cases} \Rightarrow \begin{cases} ds = -d\alpha \\ dt = -d\beta \end{cases}$

$= \int_{-\infty}^{+\infty} \int_{-\infty}^{+\infty} f(x-s, y-t) g(s,t) ds dt$

by comparison with the definition of correlation: $f(x,y) \circ g(x,y) = \int_{-\infty}^{+\infty} \int_{-\infty}^{+\infty} f(\alpha,\beta) g(x+\alpha, y+\beta) d\alpha d\beta$
we see that the convolution can be reformed to a correlation with a filter rotated at 180° . As correlation in the frequency domain can be written as $F^*(u,v) G(u,v)$ a simple product, we deduce that the most efficient computation is done in the domain

N.B: if $f = M$ non zero samples, $g = N$ non zero samples \rightarrow convolution has $M+N-1$ non zero samples as



• discrete: convolution: $f(x,y) * g(x,y) = \sum_{\alpha=-\infty}^{+\infty} \sum_{\beta=-\infty}^{+\infty} f(x-\alpha, y-\beta) f(\alpha,\beta)$

$= \sum_{\alpha'=-\infty}^{+\infty} \sum_{\beta'=-\infty}^{+\infty} f(x+\alpha', y+\beta') f(-\alpha', -\beta')$

$= \sum_{\alpha'=-\infty}^{+\infty} \sum_{\beta'=-\infty}^{+\infty} f(x+\alpha', y+\beta') f_{rot(180)}(\alpha', \beta')$

correlation: $f(x,y) \circ g(x,y) = \sum_{\alpha=-\infty}^{+\infty} \sum_{\beta=-\infty}^{+\infty} g(x+\alpha, y+\beta) f(\alpha,\beta)$

$\rightarrow (2M+1) \times (2N+1)$ mask

\rightarrow convolution of 2 3×3 mask $\rightarrow 5 \times 5$ mask

\rightarrow lin. slide 26 - 27 - 28

• composed convolution: $f_{filt_1}(x,y) \circ (f_{filt_2}(x,y) \circ im(x,y)) = (f_{filt_1}(x,y) * f_{filt_2}(x,y)) \circ im(x,y)$

$f_{filt_1}(x,y) * f_{filt_2}(x,y) \circ im(x,y)$

$\bullet FILT_1(u,v) (FILT_2(u,v) \cdot im(u,v)) = (FILT_1(u,v) \cdot FILT_2(u,v)) \cdot im(u,v)$

Lowpass filtering

It allows to reduce the noise variance, at the expense of distorting the signal by reducing the high frequency components while preserving the low frequency components. The larger the mask is, the less we detect edges and the more is their exact location evaluated. Typical masks are:

PSF  $1/3$

1	1	1
1	1	1
1	1	1

 $1/10$

1	1	1
1	2	1
1	1	1

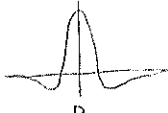
 $1/16$

1	2	1
2	4	2
1	2	1

 EXAM: explain

Unsharp masking

It accentuates the high frequency components of the image. The sum of the coefficients is one. This characteristic has the effect of preserving the average intensity of the original image in the filtered image. The edges are little highlighted but the background more has been increased because it has typically significantly high frequency components.



0	-1	0
-1	5	-1
0	-2	0

1	-2	2
-2	5	-2
1	-2	1

 $1/2$

-1	-2	-2
-2	13	-2
-2	-2	-1

Unsharp masking is closely related to highpass filtering. It is the general process of adding a highpass filtered version of an image to a fraction of the original image:

$$\text{unsharp} = (\alpha - 1) * \text{original} + \text{highpass}$$
 such that $\sum \text{highpass components} = 0$ and $\sum \text{unsharp components} = 1$
If $\alpha = 1 \rightarrow$ identical highpass result, if $\alpha > 1$, part of the original image is added to the highpass result, which partially restores the low frequency components lost in the highpass filtering operation. As a result, the image after unsharp masking looks more like the original image, with a relative degree of edge enhancement that depends on the value of α .

A highpass filter


-1	-1	-1
-1	8	-1
-1	-1	-1


 an unsharp mask with $w = 9\alpha - 8$ and $\alpha > 1$ $1/3$

-1	-1	-1
-1	W	-1
-1	-1	-1

Median filtering

The median filter is a non-linear filter. It replaces the value of the pixel located at the center of the moving mask by the median of the gray values of the pixel inside the mask. The goal is to reduce impulse or salt-and-pepper noise (edge invariant size to width of the spikes and their density ??), preserves edges &

 1) sort: $b < a < c$
2) replace center value (1) by median value c : $b \rightarrow a$

while reducing random noise and preserve corners (aka sharp window shape ??)
Example: slide 33, the 3 pixels median filter doesn't work because when the filter is center on  the median value sensitivity is always \square
 \rightarrow solution: increase filter size.

Median filter is characterized by smoothness on the edge.

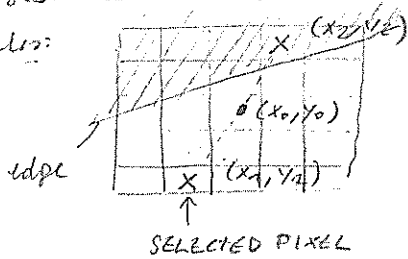
Symmetric nearest neighborhood

This type of filter can detect an edge and select the pixel that are supposed to be filtered such that it doesn't filter the edge out. The goal is to flatten the interior of regions upon while at the same time enhancing blurred edges. It does this by selecting the pixels as such, supposing that the mask is centered at pixel (x_0, y_0) :

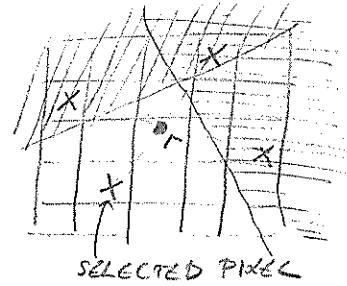
- if $|f(x_0, y_0) - f(x_1, y_1)| < |f(x_0, y_0) - f(x_2, y_2)| \rightarrow \text{select } f(x_1, y_1)$
- if $|f(x_0, y_0) - f(x_1, y_2)| > |f(x_0, y_0) - f(x_2, y_2)| \rightarrow \text{select } f(x_2, y_2)$
- if $|f(x_0, y_0) - f(x_1, y_2)| = |f(x_2, y_0) - f(x_2, y_2)| \rightarrow \text{select } f(x_0, y_0)$

and the value of the pixel at position (x_0, y_0) is replaced by the mean or median of the selected values.

Examples:



or filter preserving edges
interval of 90°
(looks at 4 positions at
same time)



PSEUDO COLORING

The gray scale image is transformed to a colour image (e.g. by mapping each gray level or a range of levels onto a different colour, which is called pseudo colour). The advantages are that the coloured image enables easier identification of pixels having different gray values. Also, colours draw quick identification of all regions in the image having the same pixel values. The disadvantages are usually destroys the spatial pattern of image (false contours might be created, viz. similar gray values can get completely different colours).